

LONG-TERM TRENDS IN THE AGE AND SIZE STRUCTURE OF  
MARINE FISHES

by

Julie Aimée Charbonneau

Submitted in partial fulfillment of the requirements  
for the degree of Master of Science

at

Dalhousie University  
Halifax, Nova Scotia  
August 2020

© Copyright by Julie Aimée Charbonneau, 2020

*Dedicated to Vincent & Sheila Charbonneau.*

# Table of Contents

List of Tables . . . . .	v
List of Figures . . . . .	vii
Abstract . . . . .	ix
List of abbreviations used . . . . .	x
Acknowledgements . . . . .	xi
<b>Chapter 1 Introduction . . . . .</b>	<b>1</b>
<b>Chapter 2 Rebuilding age structure in global marine fisheries . . . . .</b>	<b>4</b>
2.1 Introduction . . . . .	4
2.2 Methods . . . . .	6
2.2.1 Data sources . . . . .	6
2.2.2 Data analysis . . . . .	6
2.2.2.1 Prewhitened cross-correlations . . . . .	6
2.2.2.2 Simulations . . . . .	9
2.2.2.3 Regressions . . . . .	9
2.3 Results . . . . .	10
2.3.1 Temporal patterns in age structure . . . . .	10
2.3.2 Simulations: testing the utility of prewhitened cross-correlations . . . . .	11
2.3.3 Other factors affecting age structure . . . . .	12
2.4 Discussion . . . . .	12
2.4.1 Drivers underlying observed trends . . . . .	15
2.4.2 Mechanisms and implications of changing age structure . . . . .	17
2.4.3 Managing for age structure . . . . .	19
2.5 Conclusions . . . . .	19
<b>Chapter 3 Pervasive declines in monkfish (<i>Lophius americanus</i>) size structure throughout the northwest Atlantic . . . . .</b>	<b>23</b>
3.1 Introduction . . . . .	23
3.2 Methods . . . . .	25
3.2.1 Study area . . . . .	25

3.2.2	Data sources . . . . .	26
3.2.2.1	DFO survey . . . . .	26
3.2.2.2	NEFSC survey . . . . .	26
3.2.2.3	Data used for the analysis . . . . .	27
3.2.3	Statistical analyses . . . . .	28
3.2.3.1	All subareas . . . . .	28
3.2.3.2	Canada-US bottom trawl survey comparison . . . . .	29
3.3	Results . . . . .	29
3.3.1	Temporal patterns in size structure . . . . .	29
3.3.2	Spatial patterns in size structure . . . . .	30
3.3.3	Other factors affecting size . . . . .	32
3.3.3.1	Gear . . . . .	32
3.3.3.2	Season, temperature and depth . . . . .	33
3.4	Discussion . . . . .	33
3.4.1	Inter-country discrepancies in size-selectivity . . . . .	33
3.4.2	Drivers underlying the observed trends . . . . .	34
3.4.3	Implications of decreasing body size . . . . .	37
3.5	Conclusions . . . . .	37
<b>Chapter 4</b>	<b>Conclusion . . . . .</b>	<b>42</b>
	<b>Bibliography . . . . .</b>	<b>43</b>
	<b>Appendix SA . . . . .</b>	<b>52</b>
	<b>Appendix SB . . . . .</b>	<b>56</b>

## List of Tables

1	Stocks included in the analyses: unique stock identifier, management agency, taxonomy (i.e. order, genus, species), average age and average $F/F_{MSY}$ of each stock, percentage of the time-series that the stock was above (overfish) or below $F/F_{MSY}$ , time-series properties (i.e. first and last years of data and total time-series length). . . . .	21
2	Results from simulations (2.2.2) where, different properties of the time-series are set: variance in $F/F_{MSY}$ and age, the lag and the correlation (representing a specific quadrant) and time series length. The resulting significant correlations (sig.quadrant, LL: lower left, UR: upper right, UL: Upper left, LR: lower right) and strongest signal (abs.quadrant) are displayed. The proportion in the correct quadrant indicates how many (out of 1000 simulations) of the strongest signals are in the correct quadrant. The proportion correct lag indicates how many of the former are at the correct lag value. The average correlation at the correct lag (blue dot in figure 2) is calculated, with the associated standard deviation (sd). Finally, the difference between the set correlation and the average is calculated (spread between red and blue circles in figure 2). . . . .	22
3	Specifications and spatiotemporal coverage of gear used in the analysis. GOM=Gulf of Maine, GB=Georges Bank, BOF=Bay of Fundy and SS=Scotian Shelf. Nb: Canada and the United States divide survey seasons differently. In the analysis the seasons are divided such that: fall=September-December, spring=January-May, summer=June-August. . . . .	39
4	Spatiotemporal coverage of surveys in Canada and the United States. Where GOM=Gulf of Maine, GB=Georges Bank, BOF=Bay of Fundy, SS=Scotian Shelf and observations are individual length frequencies. . . . .	40
5	Relative support for linear mixed effects models tested in equation 1. Monkfish length (cm) as a function of different fixed effect predictors with a random slope of year and random intercept of area, where df represents degrees of freedom, LogLik is the log likelihood, $\Delta$ AIC is the relative difference in Akaike Information Criterion and wi are the Akaike weights . . . . .	41

SA1	Relative support for linear models tested in analysis 2.2.2.3. Correlation and lag (from strongest signal) in the lower left (LL) and upper right (UR) quadrants as a function of different fixed effect predictors. df represents degrees of freedom, $\Delta$ AICc is the relative difference in Akaike Information Criterion corrected for small sample size and r2 is the adjusted coefficient of determination from a least-squares model. . . . .	53
SA2	Results from the prewhitened cross-correlations (analysis 2.2.2.1). The upper 90 % C.I. value, correlation (cor), lag and significance (sig) per quadrant (UR= upper right, LR= lower right, UL= upper left, LL= lower left) and ARIMA orders (p,d,q) are represented for each stock. . . . .	54
SA3	Details for prewhitened cross-correlation analysis 2.2.2.1. . . . .	55
SB1	Estimated regression parameters, standard errors and t-values for the mixed effects model presented in equation 1. Baselines for gear type = Yankee trawl and for season = summer. The estimated value for $\sigma_{Year}=0.06128$ and $\sigma_{Area}=49.44346$ . . . . .	58
SB2	Estimated regression parameters, standard errors, t-values and p-values for the linear model presented in equation 2. Baseline gear type = Yankee trawl. . . . .	59
SB3	Relative support for linear models tested for the US-Canada bottom trawl survey comparison (equation 2). Monkfish length (cm) as a function of different fixed effect predictors, where df represents degrees of freedom, LogLik is the log likelihood, $\Delta$ AIC is the relative difference in Akaike Information Criterion, wi are the Akaike weights and r2 is the coefficient of determination from a least-squares model. . . . .	60

## List of Figures

1	Time series of $F/F_{MSY}$ (input) and age (output) for an ICES <i>Pleuronectes platessa</i> stock and associated correlogram following prewhitening. Significant correlations (at associated lag $K$ position) fall outside of the blue striated line (90% C.I.) . . . . .	8
2	Results from the prewhitened cross-correlations (analysis 2.2.2.1). Each circle is representative of stock, where blue dots represent a significant correlation, and red dots indicate the strongest signal (absolute maximum correlation). . . . .	11
3	Results from a selection of simulation models (2.2.2, Table 2), where grey circles represent any correlation (at associated lag point) in the targeted quadrant (fishing or management depending on the model). Red circles represent the expected correlation (sensitivity) and lag (response) value, compared against blue circles that represent the actualized mean correlation. The higher the spread between these two values, the weaker the signal detection. . . . .	13
3.1	The results from a selection of simulated prewhitened cross-correlations (2.2.2, Table 2) under low (model 1) vs. high variance (model 4) is displayed compared to target value illustrated in red. The effect of correlation strength is demonstrated by displaying the results from model 1 (high, -0.9), model 14 (medium, -0.5) and model 15 (low, -0.3), compared to the target values (colour coded by category). Both panels represent the fishing scenario. . . . .	14
4	Map of study area. Shaded areas represent the four areas broadly encompassed in the study: the Scotian Shelf (SS) and the Bay of Fundy (BOF), the Gulf of Maine (GOM), and Georges Bank (GB). The dashed line represents the Canadian EEZ. NEFSC statistical areas and DFO survey strata are included for illustrative purposes. . . . .	25
5	Partial residuals of modelled monkfish length frequencies (equation 1) for each respective gear type (US: Yankee trawl, Modified Yankee trawl, scallop dredge; Canada: Western IIA trawl) with slopes and 95 % confidence intervals superimposed. Note model is centered, where year 0 is 1981. . . . .	30

6	Map of study area. Shaded areas represent BLUPs (standard deviations from the Canadian (DFO) and US mean (NEFSC)) n=70, where positive and negative intercepts and slopes are represented and shaded according to scale and areas with values of 0 are shaded grey. The dashed line represents the Canadian EEZ. NEFSC statistical areas and DFO survey strata are included for illustrative purposes. . . . .	31
7	Effect size plot from a linear mixed model analysis of monkfish length frequencies n=20,290 across Canada and the United States (US: Yankee trawl, Modified Yankee trawl, Scallop dredge; Canada: Western IIA trawl). Circles represent the estimates, thick and thin bars represent 90 % and 95 % uncertainty intervals, respectively. Positive values correspond to increased length relative to the baselines (gear type: Yankee trawl, season: summer). Year centered at 1981. . . . .	32
SA1	Stock-specific time series of $F/F_{MSY}$ and age, residuals and correlogram from analysis 2.2.2.1. . . . .	52
SB1	Effect size plot from a linear model analysis of monkfish length frequencies n=678 for the US-Canada bottom trawl survey comparison (equation2) (US: Yankee trawl, Canada: Western IIA trawl). Circles represent the estimates, thick and thin bars represent 90 % and 95 % uncertainty intervals, respectively. Positive values correspond to increased length relative to the baseline gear type (i.e. Yankee trawl). Year centered at 2007 .	57



## Abstract

The phenotypic plasticity of marine fishes can generate demographic changes in response to harvesting, the environment, and interspecific interactions. Shifts in age and size can affect metrics of population viability related to reproduction, growth, and survival. This thesis involved the analysis of large-scale temporal trends in age and size structure of exploited fish stocks. In Chapter 1, the examination of 43 stocks allowed for the evaluation of sensitivity and response time in age structure to historic levels of fishing mortality. Significant responses were exhibited in 88% of stocks, attributed to fishing or management. Chapter 2 investigated changes in northwest Atlantic monkfish (*Lophius americanus*) size structure, finding a 48% reduction in body length over 55 years, with the average length of fish affected by survey gear, temperature, and depth. A better understanding of the causes and consequences of these shifts improves our ability to predict and mitigate future changes.

## List of abbreviations used

$F$	Fishing mortality
TAC	Total Allowable Catch
NOAA	National Oceanic and Atmospheric Administration
NEFSC	Northeast Fisheries Science Center
AFSC	Alaska Fisheries Science Center
ICES	International Council for the Exploration of the Sea
NAFO	North Atlantic Fisheries Organization
$F_{MSY}$	$F$ rate consistent with achieving a maximum sustainable yield
ARIMA	Integrated Moving Average
LL	Lower left
UR	Upper right
UL	Upper left
LR	Lower right
AIC <sub>c</sub>	Akaike's Information Criterion for small sample size
SD	Standard deviation
US	United States
DFO	Department of Fisheries and Oceans
SS	Scotian Shelf
BOF	Bay of Fundy
GOM	Gulf of Maine
GB	Georges Bank
ICNAF	International Commission for the Northwest Atlantic Fisheries
REML	Restricted maximum likelihood
BLUP	Best linear unbiased prediction
ABC	Acceptable biological catch

## Acknowledgements

First and foremost, I would like to thank my co-supervisors Dr. Jeffrey Hutchings and Dr. David Keith for their encouragement, guidance, and vision. I am immensely grateful for their support and the wonderful opportunities they provided. I am also thankful for the counsel and insightful discussions with both of my committee members Dr. Aaron MacNeil and Dr. Nancy Shackell.

I was fortunate to have been surrounded by such a brilliant and encouraging group of lab mates. It has been a pleasure spending time together, both in and outside of the lab. Thank you to Raphaël McDonald, Sean Godwin, Sebastián Pardo and Carmen David for their invaluable support in teaching me about statistics and R. I have really enjoyed the coffee chats and hangouts (more recently virtually) with everyone, including Melanie Massey, Manuelle Beaudry-Sylvestre, Kate Medcalf and Kayla Hamelin.

One of my favourite parts of the last two years has been being a part of the Scallop Unit at the Bedford Institute of Oceanography (Jessica Sameoto, Dave Keith, Freya Keyser, Andrew Taylor, Tricia Pearo Drew and Jamie Raper). A huge thank you for taking me in as your own and for giving me an appreciation of the complex world of stock assessments and fisheries management.

Finally, I would like to thank my family and friends for their unwavering support.

# Chapter 1

## Introduction

Communities are structured by complex collections of interacting organisms. Since Darwin's theoretical framework for understanding the origin of species by natural selection, much work has been devoted to characterizing the life-history differences between populations within species, especially since Fisher's (1930) [39] theoretical frame for life-history evolution. Differences in life-history have since served as a foundation for understanding variation in fish populations, with the goal of developing management frameworks aimed at meeting long-term needs. Considerably less attention has been directed towards understanding intraspecific trait variation, which has the potential to profoundly alter community dynamics and the ecosystem goods and services they provide.

Fisheries present a unique opportunity to study these shifts, as the global landscape of marine resources is changing rapidly, through a long-standing history of exploitation and environmental change. Harvesting shapes natural communities by targeting a component of a stock (i.e. the biologically-based management unit). Conventionally the target has been older and larger fish [89, 95]. Disproportionately removing part of the stock increases the proportionate contribution of recruits by the remaining population components. Combined with the plasticity of marine teleosts [83], this can result in changes in traits related to age, growth, maturity and reproduction [44, 28]. The manner in which stocks have been exploited over time has changed considerably. Global catches peaked in the mid-1980s, followed by unprecedented changes in fishery management and reformation [75, 14].

The present work examines long-term trends in age and size of commercially exploited fish populations or stocks. These traits are related to a multitude of biologically and behaviourally important functions that dictate individual ability to reproduce and respond to environmental variability [4]. The effects of fishing interact with unique life histories, community dynamics and the environment, thus affecting

the overall productivity of the stock. Disentangling these interactions and seeking to better understand the causes and consequences of intraspecific life-history shifts contributes to the development of an increasing number of fisheries management strategies directed towards sustainability.

### **Chapter 2 overview :**

Abstract: Marine fisheries have a long-standing history of exploitation. Combined with selective properties, they have the potential to shape many life-history traits, particularly those that are heritable, such as age and size at maturity. This can lead to demographic changes in the stock, often hypothesized to result in earlier age and smaller size at maturity. Many benefits are conferred by having a broad age structure, including extending the spatiotemporal spread of spawning and increasing stability and resilience in variable or unfavourable environmental conditions. Here, we study 43 marine fish stocks, using prewhitened cross-correlations (removing autocorrelation in either series), to examine the relationship between historical levels of fishing mortality and shifts in age structure. Widespread responses were evident, with 88 % of stocks being associated with fishing pressure. For 37 % of stocks, changes in age structure followed increases in fishing mortality, whereas changes in the age structure of 39 % of stocks preceded changes in fishing pressure. Sensitivity and response time varied widely, likely a result of management, exploitation, and life-history. The efficacy of this method was tested empirically by simulations, revealing that certain time-series properties (e.g. high variance and low strength correlation) have the potential to obscure the analysis. Methods that allow for the precise identification of sensitivity and response time to pressures such as fishing contribute to the development of stock-specific management measures aimed at protecting age structure (or rebuilding) on timescales that are meaningful to fisheries managers, bringing us closer to achieving sustainability targets.

### **Chapter 3 overview:**

Abstract: Shifts in size structure have been documented for many commercially exploited marine fish stocks, thought to be attributed to size-selective harvesting practices coupled with changing oceanic conditions. Northwest Atlantic monkfish (*Lophius americanus*) is a commercially valued species in the United States that is commonly

caught as bycatch in Canadian scallop and groundfish fisheries. This uniquely positioned stock is bisected by the Canadian-American jurisdictional boundary, with considerable differences in exploitation and management across its range. The status of this species was assessed nearly two decades ago (2000) in the Maritimes region of Canada and more recently (2016) in the United States, with both countries reporting considerable decreases in the average and maximum size attained by fish. A comprehensive understanding of the magnitude of this size decrease and the drivers underlying these changes across this species' range is lacking. Here, using 55 years of fishery-independent survey data, we apply a linear mixed effects model to quantify temporal changes in monkfish length frequencies. Widespread decreases were evident in both countries, with a 48 % reduction in historic body length, indicating that the large fish once prevalent in the 1970s have become uncommon. Length varied significantly as a function of seasonality and bottom temperature. Discrepancies exist in the average observed size between countries when controlling for year, season, and area; with monkfish observed by the United States trawl survey 6 cm larger on average than those observed by the Canadian trawl survey. The implications of this difference should be considered when combining fish length data from multiple surveys. Irrespective of survey differences, the truncation of size structure in Northwest Atlantic monkfish is significant and understanding how these drivers, among others hypothesized to affect size structure (e.g. fishing mortality, density dependence), are associated with population viability will be necessary to ensure its long-term sustainability.

## Chapter 2

### Rebuilding age structure in global marine fisheries

#### 2.1 Introduction

Marine fisheries have been harvested for millennia, leading to the expansion of international trade, the development of economies and increased food security, with many species holding strong cultural significance. The manner in which stocks have been fished has changed over time, and species such as Atlantic cod (*Gadus morhua*), Atlantic herring (*Clupea harengus*), bluefin tuna (*Thunnus thynnus*), and European pilchard (*Sardina pilchardus*) were heavily exploited prior to industrialization [54]. After this period, the global seafood trade expanded, along with the specialization of fishing gear and technology, in response to an increased demand for seafood [54]. Fisheries were once considered common property and their perceived inexhaustibility pervaded fisheries science for the latter half of the 19th century [71]. We now know this to be false, with this type of mentality contributing to the collapse of fisheries around the globe (e.g. Northern cod [*Gadus morhua*] in 1992; [69]).

It is widely accepted that the selectivity of marine fisheries, in conjunction with periods of long fishing, have the potential to profoundly influence stock dynamics [60]. These characteristics of fisheries, coupled with the phenotypic plasticity of teleosts can lead to demographic changes [77, 62]. Shifts have been documented for traits associated with moderately high heritability, such as age and size at maturity [44, 59]. Preserving a diverse age structure has been hypothesized to increase population stability and resilience, with older individuals contributing differentially to reproduction in both the spatiotemporal spread of spawning and the viability of larvae produced [87, 16, 68, 47, 12]. Harvest-induced truncations in age structure have been documented for several marine fish stocks [49, 85, 94, 5], potentially altering their ability to cope with ongoing environmental changes.

Fishery management practices have changed over time, partly resulting from an

increased understanding of how harvesting impacts life-history traits [50]. Global fishing intensity peaked in the mid-1980s [75]. The resulting collapses motivated many countries to make sustainability commitments and heighten their management measures [45]. To a large extent, approaches involve enforcing harvest within the limits of scientifically determined reference points, resulting in widespread declines in fishing mortality ( $F$ ) after this period for well-managed stocks [37]. Key fishery reforms include the Magnuson-Stevens Act in the United States (1976), the Common Fisheries Policy in Europe (1982), and enforcement of Total Allowable Catches (TACs) in Japan (1997), all of which were facilitated to greater or lesser degrees by the 2020 Aichi target of rebuilding depleted fish stocks established by the Convention on Biological Diversity [14].

Much work has been dedicated to understanding how increased exploitation affects commercially valuable marine fish stocks. Comparatively less research has been devoted to understanding the reversibility of changes attributed to exploitation and stock-specific rebuilding potential. Addressing these questions has become possible with the widespread fishery reformations occurring in recent decades. Predicting the sensitivity and response time to these changes will be necessary to assess the efficacy of instituted management measures. Cross-correlations may serve to investigate the lagged temporal relationship between two-time series although the autocorrelation present in many fisheries data have has the potential to confound the analysis. Prewhitening has been suggested as a technique to resolve this issue and reduce spurious correlations [79]. In the present study we : (i) conduct a time-series analysis in conjunction with prewhitened cross-correlations to examine temporal relationships between  $F$  and age structure; (ii) examine stock-specific differences in sensitivity and response time, along with potential drivers responsible for the associated trends; and (iii) undertake simulations to determine how the methodology is affected by the properties of a coupled time-series.



## 2.2 Methods

### 2.2.1 Data sources

Age-specific, temporal metrics of abundance and  $F$  were compiled for 43 commercial marine fish stocks, from a subset of a data compiled by Charbonneau et al. (2019) [22]. Data were sourced from publicly accessible stock assessments published by national and international entities: United States (NOAA, National Oceanic and Atmospheric Administration: including the Northeast Fisheries Science Center [NEFSC] and the Alaska Fisheries Science Center [AFSC]), Europe (ICES, International Council for the Exploration of the Sea), and Northwest Atlantic waters that straddle international boundaries (NAFO, North Atlantic Fisheries Organization). Abundance at age provided in the assessments are either sourced from survey indices or model estimates when survey indices were not available. The  $F$  rate consistent with achieving a maximum sustainable yield ( $F_{MSY}$ ) was extracted from stock assessments and the RAM III Legacy database (ramlegacy.org). The data represent 20 species from five taxonomic orders: Pleuronectiformes, Gadiformes, Clupeiformes, Scombriformes and Perciformes. Additional details are presented in Table 1.

### 2.2.2 Data analysis

#### 2.2.2.1 Prewhitened cross-correlations

The relationship between two series distributed over time can be interpreted by cross correlations. This tool allows for the evaluation of stock-specific sensitivity (correlation) and responsiveness (lag  $K$ ) of a state indicator (e.g. age) in response to a pressure (e.g. fishing mortality).

First, the mean age for each stock in year  $t$  ( $\bar{A}_t$ ) was calculated:

$$\bar{A}_t = \frac{\sum_1^a (A_x \times N_{x,t})}{\sum_1^a N_{x,t}} \quad (1)$$

where  $A_x$  is the age of age group  $x$  and  $N_{x,t}$  is the number of individuals in age group  $x$  in year  $t$ . Fishing mortality for each stock in year  $t$  was standardized by  $F_{MSY}$  to facilitate comparison between stocks by accounting for inter-specific differences in

response time. Both age and  $F$  were centered and standardized with deviations measured in units of standard deviations. Autocorrelation is a common property of time-series, where underlying trends can conceal the detection of the strongest signal and the interpretation of the relationship between cross-correlated series. As such, this method requires each time-series to be stationary (i.e. the mean and variance remain unchanged through time). This can be accomplished by using Autoregressive Integrated Moving Average (ARIMA) models in conjunction with prewhitening, whereby the removal of spurious autocorrelations allows for identification of key significant correlations and lags that might otherwise be undetected in the unprocessed series.

The hypothesized relationship between two series determines the order of the input and output series; in this case  $F$  (input series) is expected to lead changes in average age (output series). Prewhitening is attained by fitting an ARIMA model to the input, which is subsequently applied to the output. These integrated models with the notation ARIMA(p,d,q) combine autoregressive (AR, p) and moving average (MA, q) components with differencing (d). Additional information detailing this process and resources can be found in Table SA3. The residuals from this model were calculated (prewhitening) and the same model was applied to the output series (age) to achieve the prewhitened state. These were used to tabulate cross-correlations among the two series. The strongest signal (maximum absolute correlation) and associated lag was extracted from each quadrant in the correlogram.

The position of the significant lag and associated correlation in the correlogram allows for the inference of stock-specific pressure-state relationships (Figure 1). This information can then be implemented to evaluate the effectiveness of potential management strategies aimed at conserving desired traits. The utility of this approach in the context of pressure-state relationships for ecosystem-based management is discussed by Probst et al. (2012) [79]; additional information can be obtained therein.

The analysis was repeated using a subset of data beginning in both 1975 and 1980 to ensure that the results were not unduly influenced by early years when survey effort was comparatively lower than in recent times. Additionally, a subset examining fish five years and older was performed to determine if the exclusion of young age classes influenced these results (i.e. recruitment).

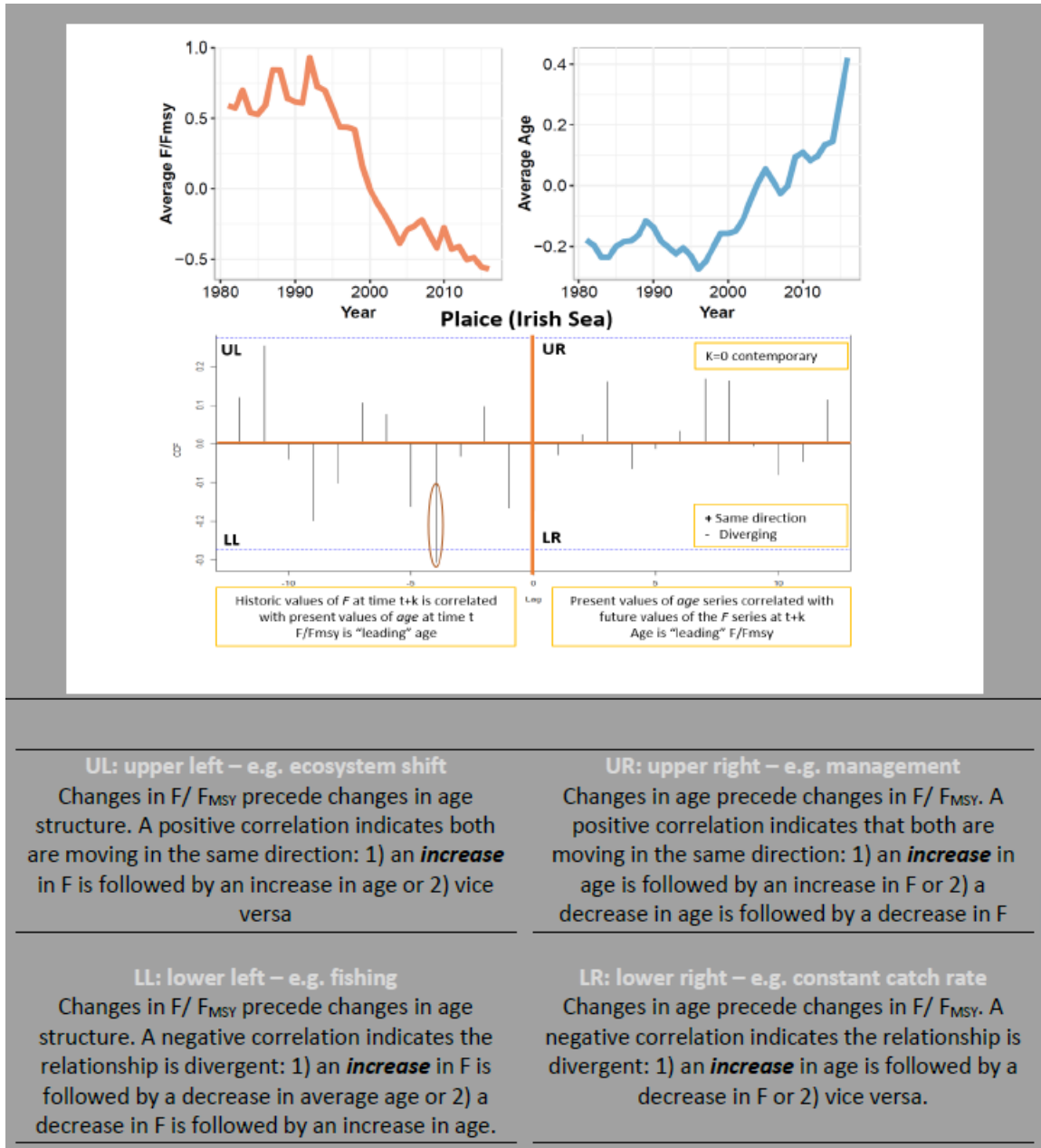


Figure 1: Time series of  $F/F_{MSY}$  (input) and age (output) for an ICES *Pleuronectes platessa* stock and associated correlogram following prewhitening. Significant correlations (at associated lag  $K$  position) fall outside of the blue striated line (90% C.I.)

### 2.2.2.2 Simulations

The efficacy of this methodology was tested by undertaking an analysis using simulated data. The input and output time-series representing fishing pressure and age were generated by setting specific parameters to simulate different time-series characteristics. Twenty different scenarios were tested (Table 1), in each case by generating 1000 different replicates and conducting the analysis detailed in section 2.2.2.1. The baseline parameter values used to create the replicates were chosen based on data from the input and output series in 2.2.2.1. This included the highest and lowest variance values exhibited in the data, combinations of which were tested in the base models for the fishing (models 1-4, Table 2) and the management (models 4-8) scenarios. The strength of correlation was initially set with a high value ( $\pm 0.9$ ), and subsequently tested with values representative of the data (i.e.  $\pm 0.5$  and  $\pm 0.3$ ). The average lag value was  $\pm 4$  and the length of data was 38 years, both of which were adjusted based on the model. This served to evaluate the effect of several time-series properties: mean and variance, ARIMA parameters (length of lag, strength of correlation) and the length of the series affected the reliability of the method insofar as detecting the appropriate signal (i.e. the strongest correlation located in the appropriate quadrant).

### 2.2.2.3 Regressions

The correlation and associated lag value for the strongest signal in both the “fishing” LL and “management” UR scenarios (2.2.2.1) were used as response variables in a suite of linear models examining correlates responsible for the sensitivity and response time of the pressure-state relationship between  $F$  and age. These included management agencies, taxonomy, environment (i.e. benthic, pelagic), fishing intensity and lifespan. Fishing intensity was divided into two categories (“high” and “low”) based on the percentage of the time-series during which  $F$  was above ( $\geq 50\%$  [overfishing occurring]) or below  $F_{MSY}$  ( $< 50\%$  [fished under  $F_{MSY}$  limit]). Management agencies were grouped into: ICES, NEFSC, AFSC and “other” based on the number of stocks falling into each category. Lifespan was categorized into two groups, “young” (6-10 years) and “old” (11-20 years), based on the maximum age for which abundance data were available (note these tend to be lower than absolute maximum ages as stock assessments employ a “plus group” after which very few older fish are sampled).

Various model configurations were tested using combinations of these covariates in either scenario (Table SA1), and the relative support was determined using the Akaike’s Information Criterion for small sample size (AICc). Management agencies and orders with two or fewer observations (i.e. AFSC, Other, Scombriformes, Perciformes depending on the subset) were removed from the analyses. The “fishing” and “management” scenario subsets included 11 and 14 stocks, respectively.

## 2.3 Results

### 2.3.1 Temporal patterns in age structure

The temporal relationship between  $F$  and age structure was investigated for 43 marine fish stocks (Table 1). The median time-series length for these data was 38 years (ranging from 25-71 years). Widescale responses in age were evident with significant correlations (90 % C.I) exhibited in 88 % (n=38) of the stocks. Of those with a significant correlation 37 % (n=14) displayed the strongest correlation under the fishing scenario ( $F$  leads age) and 39 % (n=15) in the management scenario (age leads  $F$ ), making these the most common (Figure 1). The average responsiveness (i.e. lag) was 4 years ( $\pm 2.37$  SD) for the fishing scenario ranging from 2-9, with an average sensitivity (i.e. correlation) of -0.33 ( $\pm 0.062$ ), ranging from -0.27 to -0.48. Under the management scenario, the average responsiveness was 5 years ( $\pm 3.39$ , ranging from 1 to 11), and sensitivity 0.32 ( $\pm 0.0403$ , ranging from 0.21 to 0.40)(Table SA2).

The incidence of significant correlations in the other quadrants was much lower, with 11 % (n=4) of stocks exhibiting the strongest correlation in the UL and 13 % (n=5) in the LR (Figure 2). The average responsiveness was 6 years ( $\pm 2.5$ , ranging from 3 to 9) and sensitivity 0.34 ( $\pm 0.055$ , ranging from 0.28 to 0.38) for the former and 7 years ( $\pm 4.72$ , ranging from 1 to 14) and sensitivity -0.38 ( $\pm 0.068$ , ranging from -0.29 to -0.46 ) for the latter (Table SA2).

While we determined the most likely scenario based on the quadrant with the strongest signal, significant correlations may arise across multiple quadrants at once, notably when there are cycles of intensification and relaxation (Shumway, 2011). As such, the total incidence of significant correlations in a given quadrant are much

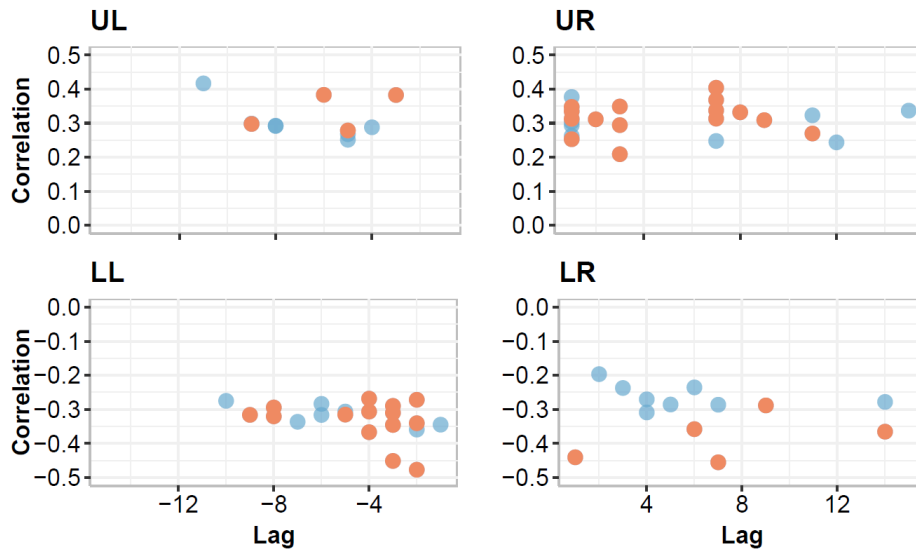


Figure 2: Results from the prewhitened cross-correlations (analysis 2.2.2.1). Each circle is representative of stock, where blue dots represent a significant correlation, and red dots indicate the strongest signal (absolute maximum correlation).

higher (Figure 2).

### 2.3.2 Simulations: testing the utility of prewhitened cross-correlations

Identifying how the exploitation history of a stock affects its age structure— thus predicting how future management frameworks might affect population viability— hinges on the ability of this method to reliably detect the strongest signal and associated quadrant. The utility of this method largely depends on specific characteristics of the data, identified by a series of simulations (Table 2). We define the accuracy of the method in its ability to identify the strongest signal (i.e. the proportion out of 1000 simulations identifying the correct quadrant and lag as defined in the baseline parameters).

The base models in the fishing (models 1-4) and management (models 5-8) tested for the effect of variance. When the expected correlation was high ( $\pm 0.9$ ), under low variance the method was over 99 % accurate with estimated average correlations of -0.78 and +0.78 (models 1 and 4), decreasing to 2 % with an average correlation of -0.36 and 79 % at 0.76 under high variance (Figure 1, Figure 3.1, models 4 and 8).

The strength of the correlation strongly influenced the accuracy, when the expected correlation was low (-0.3), under low variance the method was 34 % accurate with an estimated average correlation of -0.40 (Figure 3.1, model 15), decreasing to 0 % accuracy under high variance (model 16). Shortening the lag to -1 increased the accuracy, with the best predictor (100 % accurate) including low variance, high correlation, and short lag (model 13).

The effect of time-series length was examined in models 9-12. When the expected correlation was high (-0.9), under low variance, both the short (model 9) and long (model 10) series lengths accurately identified the correct quadrant 94 % and 100 % of the time with average correlations of -0.69 and -0.84. This decreased under high variance, -0.44 for the short series (model 11) and -0.23 for the long series (model 12), with an accuracy of 4 % for both models.

### 2.3.3 Other factors affecting age structure

Covariates affecting the stock-specific strength of sensitivity and response time for the strongest signal were investigated using four linear regression models (Table SA1). The first series investigated the fishing scenario (models A-B) and the second management scenario (models C-D), where the first models used the correlation as a response variable (models A and C), and the second using the lag (models B and D). The best models included management body and fishing intensity (models A, B, D: favoured over other configurations with a  $\Delta$  AICc of 35.5, 28.3 and 10.6 lower than the next ranked model), apart from model C ( $\Delta$  AICc 3.7 lower than next ranked model) which favoured management body and lifespan (Table SA1). Significant differences in response time were found in between ICES and NEFSC, with the age structure of the former taking 2.23 fewer years ( $\pm$  0.60, 90 % C.I.) to respond to changes in fishing mortality, under the fishing scenario (model B).

## 2.4 Discussion

The present study documents large-scale changes in age structure resulting from historic levels of fishing mortality. Across 43 stocks, 88 % exhibited significant correlations between the timing of changes in  $F$  and the timing of changes in mean age. In 37 % of the stocks, decreases in  $F$  preceded increases in average age (or vice versa,

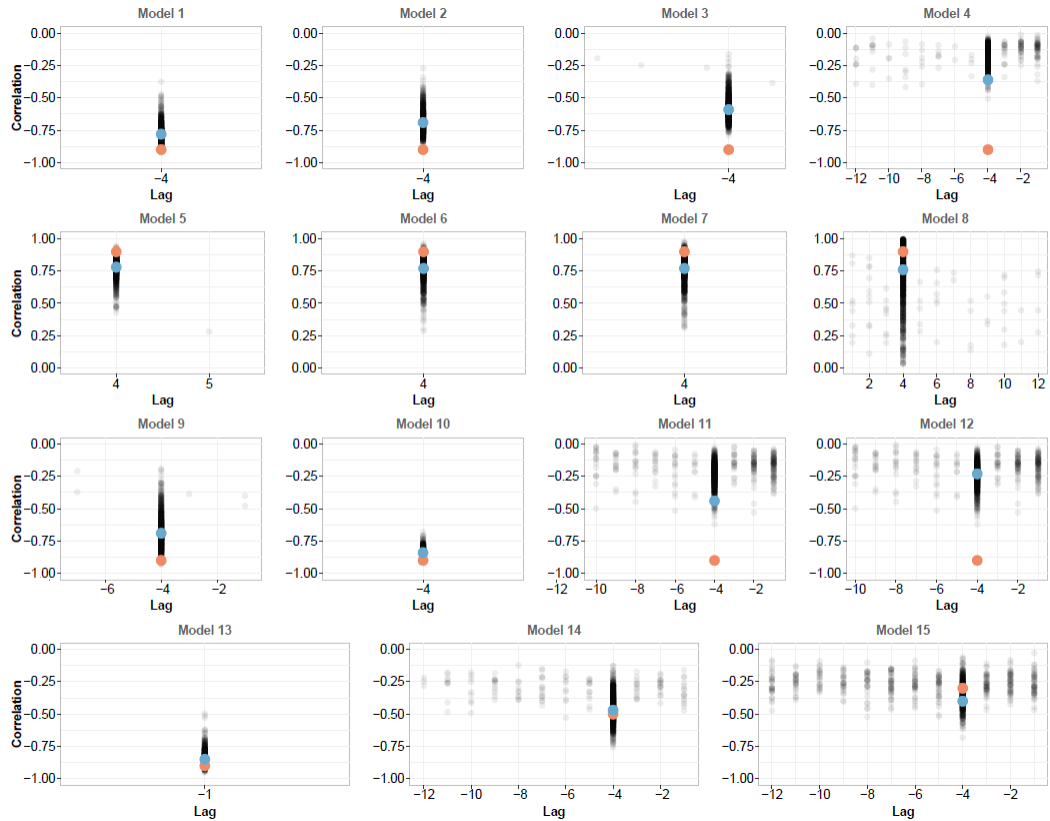


Figure 3: Results from a selection of simulation models (2.2.2, Table 2), where grey circles represent any correlation (at associated lag point) in the targeted quadrant (fishing or management depending on the model). Red circles represent the expected correlation (sensitivity) and lag (response) value, compared against blue circles that represent the actualized mean correlation. The higher the spread between these two values, the weaker the signal detection.



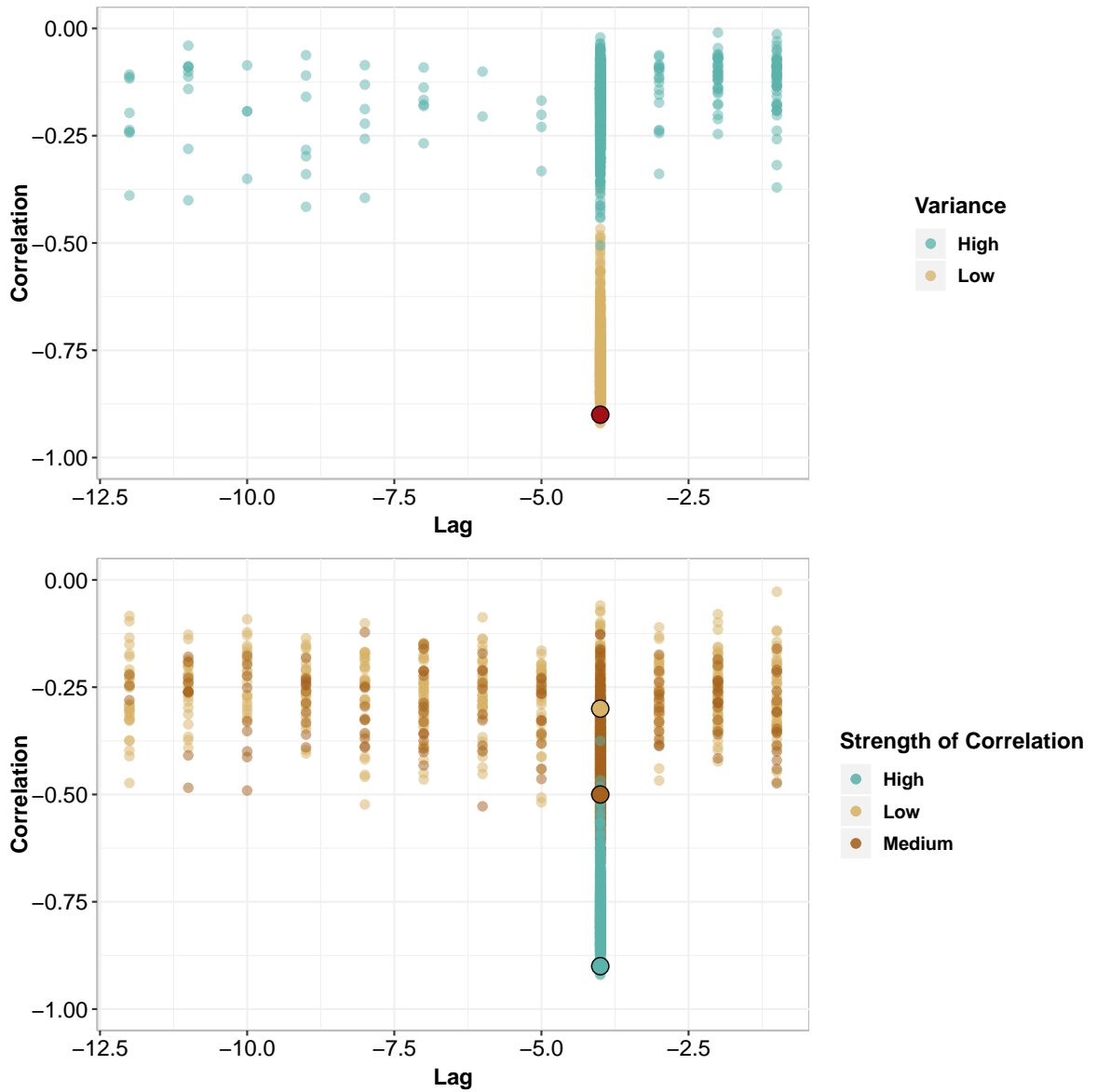


Figure 3.1: The results from a selection of simulated prewhitened cross-correlations (2.2.2, Table 2) under low (model 1) vs. high variance (model 4) is displayed compared to target value illustrated in red. The effect of correlation strength is demonstrated by displaying the results from model 1 (high, -0.9), model 14 (medium, -0.5) and model 15 (low, -0.3), compared to the target values (colour coded by category). Both panels represent the fishing scenario.

Figure 1: fishing scenario). In 39 % of stocks, increases in average age were followed by increases in  $F$  (or vice versa), suggesting that management measures may have been adjusted to account for changes in age structure—or the associated stock dynamics resulting from shifts in age structure (Figure 1: management scenario). The sensitivity and response time varied depending on the stock, likely a product of the duration and intensity of the fishery, implementation of management measures and unique life histories.

#### 2.4.1 Drivers underlying observed trends

Temporal patterns in  $F$  and the associated responses in age structure are largely driven by regulations put in place by countries and/or governing bodies, to control fishing intensity and effort (e.g. TAC, reference points, effort controls [76]). The present study reveals that sensitivity and responses to these regulatory measures are highly stock-dependent, with a wide range of sensitivities and response times that could not be generalized based on taxonomy. For example, Atlantic cod stocks showed high regional variability in sensitivity, response time, and peak correlation: 0.31, two years, "management" in the Gulf of Maine; -0.27, four years, "fishing" in the Northeast Arctic and 0.35, one year, "management", in the Celtic Sea (Table SA2, Figure SA1). The management plans for these cod stocks are centered around achieving target levels of exploitation, where levels of  $F$  are stock-dependent and subject to fluctuate interannually. The common trend for all three stocks is marked by increases in  $F$  during the development of the fishery, peak mortality occurring in the 80s-90s followed by decreases (in some cases increasing slightly in recent decades) [53, 52, 20].

The most common assessment agencies represented in the data were NEFSC (n=13) and ICES (n=26). Temporal patterns of fishing intensity reveal that 72 % of the stocks assessed in the present study had  $F > F_{MSY}$  for  $\geq 50$  % of the duration of each available time-series. Intensity and length of time that a fishery has been operating are known to affect recovery time, with stocks depleted over a short period of time ( $< 30$  years), rebuilding more slowly and less predictably than those characterized by a longer history of exploitation ( $> 50$  years) [70]. Rebuilding efforts have been made for many of the stocks assessed by these agencies, where targets revolve around

*MSY*-based reference points linked to  $F$  or biomass thresholds [68, 41, 14, 33]. ICES reports that the percentage of stocks that are overfished has dropped by 40 % from 2003 to 2016 [19]. Similarly, in 2018, NMFS (the National Marine Fisheries Service of the U.S.) reported 91 % of assessed stocks to be at or below target *MSY* limits [72]. These decreases indicate a strong potential to study rebuilding across stocks represented by these agencies. While this analysis implicitly tested for the effect of historic levels of  $F$  (fishing scenario) on average age (as parameterized by the order of the input and output series), a number of significant correlations were displayed under the management scenario, reinforcing the notion that age structure (and stock dynamics resulting from increasing/decreasing age) influences the outcome of management decisions, investment and effort deployment. There are plausible scenarios that would generate significant responses in the UL (e.g. ecosystem shift) or LR (e.g. unidirectional application of pressure), yet the incidence of strong signals was much lower in these quadrants. While prewhitening has the purpose of isolating the strongest signal, the simulations demonstrated that certain time-series properties can weaken the accuracy of the method and result in spurious correlations.

These two factors —management body and fishing intensity— were established as the most influential covariates in determining the stock-specific strength of the sensitivity and response time under the fishing and management scenarios (Table SA1). The low number of observations limits our ability to assess the relationship between covariates. Nevertheless, it strengthens the notion that these determinants strongly influence age structure, highlighting the need for customized governance.

Variability in stock-specific sensitivity and response time is influenced by time-series characteristics (Table 2, Figure 3). This was tested empirically with simulations wherein high variance and low correlation hindered the detection of the strongest signal and the ability to infer the underlying relationship between  $F$  and age. Average correlations were lower than the actual values (with the exception of model 15), implying that the sensitivity is likely higher than that displayed by the strongest signal, especially when variance is high. The average correlation for the strongest signal in analysis 2.2.2.1 was 0.3, indicating that the actualized correlation was presumably higher. With a baseline correlation of -0.5, representing a high correlation value for our data (model 13), the method was 75 % accurate. This decreased to 34 % when

the correlation was set to -0.3 (model 15). Therefore, the efficacy of the method is reduced at low correlation values but depends strongly on the characteristics of the data. Stocks for which there were no significant signal had higher variance in  $F$  on average than those displaying a strong signal, however the incidence was low ( $n=5$ ). Longer time-series were shown to improve the accuracy of this method only slightly (by 6 %, models 9 and 10). In analysis 2.2.2.1 the effect of the time-series length was negligible, indicating that the median time-series length of 39 years was likely sufficient.

While these simulations provide insight as to which general characteristics affect signal detection, realized fisheries data are complex. There are exceptions, for example a time-series may display high variance (e.g. a period of heavy exploitation followed by steep decrease), yet the strong signal renders a highly accurate detection (e.g. Figure SA1: NEFSC-SAW\_chrysops\_USATL and NEFSC-GARMIII\_dentatus\_MA ). Although it is not possible to control for the complex nature of fisheries data, these properties should all be taken into consideration when applying this method.

#### **2.4.2 Mechanisms and implications of changing age structure**

Fisheries apply selective pressure on a number of morphological, behavioural and demographic characteristics of an exploited species [83, 61]. In many cases, larger fish are preferentially selected by the gear [89, 95], as they are often of higher market value and measures are imposed to protect small fish [1]. Fish grow indeterminately, with larger individuals presumed to be older [23]. Selectively removing this part of the population would necessarily lead to decreases in average age. There is evidence that the presumed age-length relationship might be changing (e.g. several North Sea fish assemblages), especially in the last few decades, alongside factors known to affect body size, such as temperature [7]. Depending on trait heritabilities and selection intensities, the increased contribution of smaller, younger fish may lead to earlier maturation, slower growth, and reduced lifespan [62, 35]. Even unselective fishing could favour faster life histories by depreciating the value of older age classes, and consequently the advantages of delaying reproduction [43].

Evidence of age truncation has been documented for many commercially important species including Atlantic cod and herring (*Clupea harengus*) [85]. More broadly,

a study examining 63 stocks found that proportion of ages in the oldest group to have decreased significantly for 79 %, with the latest years available ranging from 2008-2016 [5]. The adverse impacts of age truncation can be manifested by reducing the population stability that is provided by having a diverse age structure [68, 47]. The spatiotemporal spread of spawning differs among old and young age classes [16, 65, 12]. In Atlantic cod, reproduction in older individuals begins earlier and is protracted compared to their younger counterparts [51]. In species such as groupers (*Epinephelus spp.*), the young follow experienced individuals to spawning aggregations [13]. The quality and quantity of larvae produced differs between age classes (e.g. haddock [*Melanogrammus aeglefinus*], Atlantic cod and bluefish [*Pomatomus saltatrix*], [13]). Older fish are presumably larger and can benefit from higher fecundity, producing larger eggs with more nutrient rich reserves, increasing starvation-resistance and fitness and making a greater contribution to the spawning-stock biomass [87, 99, 47, 11]. The benefits conferred by having a diverse age structure has been likened to a seed-bank in plants, buffering against variable or unfavourable environmental conditions [12].

While it is difficult to disentangle the effects of fishing from other factors shaping population dynamics such as per capita rate of increase, population size, density dependence, strong year classes, natural mortality, predator-prey interactions and climate—the relative impact of fishing is likely high.  $F$  often surpasses natural mortality in exploited populations [66], with the rate of phenotypic change occurring much more drastically in human-harvested systems [29].

There is evidence that age structure may be rebuilding in the last few decades for well-managed commercially harvested stocks [22, 46], as a sustained effort has been made to reform fisheries by respecting target reference points. Perhaps the greatest example of rebuilding potential occurred during World Wars I and II when sharp reductions in  $F$  were followed by a rebound in North Sea fish stocks [63, 78]. The present study provides a method of determining the timescales and sensitivity to which specific stocks may respond to  $F$ , providing insight as to how management measures may serve to preserve desired ecosystem states.

### 2.4.3 Managing for age structure

Numerous management strategies have been proposed to conserve age structure. These include: marine reserves or protected areas where fishing is prohibited [59]; slot limits enforcing minimum and maximum catch body size limits [12] and restrictions based on gear, effort, or area [5]. Many legislative frameworks that have been implemented to rebuild stocks involve respecting *MSY* reference points. The present study shows that these measures (i.e. reducing  $F$ ) may be sufficient to rebuild age structure. This should be considered in conjunction with achieving other important targets related to abundance and biomass.

The recovery of depleted stocks holds the potential for many ecological and economic benefits [27], however it is not met without challenge. Rebuilding may alter population dynamics and strengthen density-dependence, confounding the calculation of target reference points [68, 41]. This could lead to reverse trophic cascades in systems with keystone predators and increasing conflict between fisheries [97]. As a result, ecosystem-based management is increasingly suggested as holistic way of conserving ecosystem goods and services and overcome the limitations of traditional single-species stock assessment and management [33]. Providing information on a timescale that is meaningful to fishery managers (e.g. on the scale of a few years rather than decades), increases utility and the probability of implementation [50].

Using stock assessment data remains a challenge as survey effort (coverage, number of hauls) increases over time. Generally, the reliability of the data improved in the mid-1980s, following increased effort and standardization of protocols. It is also important to note the stocks examined in the present study have high FMIs (fishery management indices), many of which have been shown to be rebuilding [46]. This is not the case for many fisheries globally that have lower FMIs which are not on the same trajectory and remain heavily fished. This discrepancy can largely be attributed to resource access related to surveys, assessments, and management [68].

## 2.5 Conclusions

The present work examines the relationship between  $F$  and age structure of 43 commercially exploited marine fish stocks. Building on the work of Probst (2012)[79], we

use prewhitened cross-correlations to detect stock-specific sensitivity and response time to  $F$ , providing information that has potential to inform the growing number of management measures aimed at rebuilding and protecting age structure. The efficacy of this approach was tested empirically with simulations and found to be influenced by time-series characteristics such as length, strength of the correlation, and variability. Understanding how anthropogenic pressures affect sensitivity and response time has applications for ecosystem-based fisheries management approaches that employ indicator-based pressure-state-response frameworks to assess ecosystem health. There is considerable merit in exploring the application of this method to examine how other traits, such as size or biomass, respond to  $F$ .

Table 1: Stocks included in the analyses: unique stock identifier, management agency, taxonomy (i.e. order, genus, species), average age and average  $F/F_{MSY}$  of each stock, percentage of the time-series that the stock was above (overfish) or below  $F/F_{MSY}$ , time-series properties (i.e. first and last years of data and total time-series length).

unique_ID	mgmt	Order	Genus	Species	avg_fm <sub>SY</sub>	age	Max_age	overfish	underfish	intensity	min_year	max_year	ts_length
ICES-WGBFAS_harengus_BS 28.1	ICES	Clupeiformes	Clupea	harengus	1.12	4	25	57.89	42.11	high	1977	2015	38
ICES-WGBFAS_harengus_BS 25-29,32	ICES	Clupeiformes	Clupea	harengus	0.96	4.5	25	31.71	68.29	low	1974	2015	41
GARMIII_cynoglossus_5Y	NEFSC	Pleuronectiformes	Glyptocephalus	cynoglossus	1.97	7	25	97.06	2.94	high	1982	2016	34
ICES-WGWIDE_poutassou_NEA 1-9,12,14	ICES	Gadiformes	Micromesistius	poutassou	1.12	5.5	20	60.53	39.47	high	1981	2018	37
ICES-WGWIDE_harengus_NEA 1,2,5,6a,14a	ICES	Clupeiformes	Clupea	harengus	0.89	7	25	41.94	58.06	low	1988	2018	30
NEFSC_americanus_SZ	NEFSC	Pleuronectiformes	Pseudopleuronectes	americanus	0.93	4	14	37.5	62.5	low	1982	2014	32
ICES-WGBFAS_spratrus_BS 22-32	ICES	Clupeiformes	Spratrus	spratrus	0.97	4	6	56.1	43.9	high	1974	2015	41
ICES-WGNSSK_solea_NS 7d	ICES	Pleuronectiformes	Solea	solea	0.87	6	26	30	70	low	1982	2016	34
ICES-WGNSSK_merlangus_NS 4-7d	ICES	Gadiformes	Merlangus	merlangus	2.28	4.5	20	100	0	high	1978	2016	38
ICES-HAWG_harengus_NS-IV 3a,7d	ICES	Clupeiformes	Clupea	harengus	1.08	4	25	37.14	62.86	low	1947	2016	69
NEFSC-TRAC-CERT_morhua_GB	NEFSC	Gadiformes	Gadus	morhua	1.43	5.51	25	73.68	26.32	high	1978	2016	38
ICES-WGBFAS_solea_NS IIIa 22-24	ICES	Pleuronectiformes	Solea	solea	1.36	5.5	26	100	0	high	1984	2014	30
AFSC_macrocephalus_BSAI	AFSC	Gadiformes	Gadus	macrocephalus	1.16	10	25	63.41	36.59	high	1977	2017	40
NEFSC_scombrus_NWA	NEFSC	Scombriformes	Scomber	scombrus	1.58	5.5	17	57.14	42.86	high	1968	2016	48
NEFSC-SAW_morhua_GOM	NEFSC	Gadiformes	Gadus	morhua	3.46	5	25	100	0	high	1982	2011	29
ICES-WGSCF_solea_CS7,7g	ICES	Pleuronectiformes	Solea	solea	1.18	5	26	65.22	34.78	high	1971	2017	46
NEFSC_platessoides_5Y2	NEFSC	Pleuronectiformes	Hippoglossoides	platessoides	1.47	6	30	66.67	33.33	high	1980	2018	38
NEFSC-GARMIII_aeglefinus_5Y	NEFSC	Gadiformes	Melanogrammus	aeglefinus	0.69	5	20	21.62	78.38	low	1977	2013	36
NEFSC-GARMIII_dentatus_MA	NEFSC	Pleuronectiformes	Paralichthys	dentatus	2.34	3.5	9	74.19	25.81	high	1982	2012	30
NEFSC-GARMIII_tenuis_GOM_GB	NEFSC	Gadiformes	Urophycis	tenuis	1.84	5	23	65.31	34.69	high	1963	2012	49
ICES-WGSCF_platessa_IS27,7a	ICES	Pleuronectiformes	Pleuronectes	platessa	1.76	4.5	50	61.11	38.89	high	1981	2017	36
NEFSC-SAW_chrysops_USATL	NEFSC	Perciformes	Stenotomus	chrysops	2.57	3.5	20	51.61	48.39	high	1984	2014	30
ICES-HAWG_harengus_WBS 22-24	ICES	Clupeiformes	Clupea	harengus	1.38	4	25	76	24	high	1991	2016	25
ICES-WGSCF_solea_IS7e	ICES	Pleuronectiformes	Solea	solea	0.82	7	26	22.92	77.08	low	1969	2017	48
ICES-WGNSSK_aeglefinus_NS 9-6a-20	ICES	Gadiformes	Melanogrammus	aeglefinus	2.97	8	20	91.3	8.7	high	1965	2017	52
ICES-NWWG_virens_FASb	ICES	Gadiformes	Pollachius	virens	1.27	8.5	25	69.64	30.36	high	1961	2016	55
ICES-AFWG_morhua_NEA 1,2	ICES	Gadiformes	Gadus	morhua	1.43	8.5	25	83.1	16.9	high	1946	2017	71
ICES-WGNSSK_platessa_NS 7d	ICES	Pleuronectiformes	Pleuronectes	platessa	1.03	4	50	59.46	40.54	high	1980	2016	36
ICES-WGNSSK_platessa_NS 4,20	ICES	Pleuronectiformes	Pleuronectes	platessa	1.73	5.5	50	83.33	16.67	high	1957	2016	59
ICES-HAWG_harengus_CS 6a,7b,7c	ICES	Clupeiformes	Clupea	harengus	1.06	5	25	40.68	59.32	low	1957	2016	59
ICES-WGSCF_morhua_IS7a	ICES	Gadiformes	Gadus	morhua	2.15	3	25	89.8	10.2	high	1968	2017	49
NEFSC-GARMIII_morhua_GB	NEFSC	Gadiformes	Gadus	morhua	3.12	5.5	25	100	0	high	1978	2012	34
AFSC_aspera_EEBSAI	AFSC	Pleuronectiformes	Limanda	aspera	0.46	10.43	34	0	100	low	1975	2017	42
ICES-WGNSSK_virens_NS 4,6,3a	ICES	Gadiformes	Pollachius	virens	1.2	6.5	25	70	30	high	1967	2016	49
CERT-TRAC_aeglefinus_GB	Other	Gadiformes	Melanogrammus	aeglefinus	0.58	5	20	8.33	91.67	low	1969	2017	48
NEFSC_virens_5Y2	NEFSC	Gadiformes	Pollachius	virens	0.37	5	25	6.82	93.18	low	1970	2013	43
ICES-WGSCF_aeglefinus_ROCK6b	ICES	Gadiformes	Melanogrammus	aeglefinus	2.46	3.5	20	88.46	11.54	high	1991	2017	26
ICES-WGSCF_morhua_CS7e-8	ICES	Gadiformes	Gadus	morhua	1.8	4	25	93.48	6.52	high	1971	2017	46
NEFSC-GARMIII_ferruginea_SNE_MA	NEFSC	Pleuronectiformes	Limanda	ferruginea	3	3.5	12	89.74	10.26	high	1973	2011	38
ICES-NWWG_morhua_FAPL5d1	ICES	Gadiformes	Gadus	morhua	1.65	5.5	25	89.47	10.53	high	1959	2016	57
ICES-WGSCF_merlangus_CS7a	ICES	Gadiformes	Merlangus	merlangus	4.14	4	20	100	0	high	1980	2017	37
ICES-AFWG_aeglefinus_NEA 1,2	ICES	Gadiformes	Melanogrammus	aeglefinus	1.2	8	20	66.18	33.82	high	1950	2017	67
AFSC_polyxystra_EEBSAI-Females	AFSC	Pleuronectiformes	Lepidopssetta	polyxystra	0.19	10.5	18	0	100	low	1980	2016	36



Table 2: Results from simulations (2.2.2) where, different properties of the time-series are set: variance in  $F/F_{MSY}$  and age, the lag and the correlation (representing a specific quadrant) and time series length. The resulting significant correlations (sig-quadrant, LL: lower left, UR: upper right, UL: lower right) and strongest signal (abs\_quadrant) are displayed. The proportion in the correct quadrant indicates how many (out of 1000 simulations) of the strongest signals are in the correct quadrant. The proportion correct lag indicates how many of the former are at the correct lag value. The average correlation at the correct lag (blue dot in figure 2) is calculated, with the associated standard deviation (sd). Finally, the difference between the set correlation and the average is calculated (spread between red and blue circles in figure 2).

Mod #	F var	Age var	FM var	Age var value	Age var value	Quadrant	Lag	Corr	TS length	sig LL	sig UR	abs LL	sig UR	abs UR	sig UL	abs UL	sig LR	abs LR	Correct quad	Correct lag	Accurate signal out of 1000	Avg corr for correct lag	sd corr for correct lag	Spread
1	low	low	low	0.01	0.03	LL	-4	-0.9	38	1000	988	405	0	272	0	256	0	1.00	1.00	0	-0.78	0.07	0.12	
2	low	high	low	0.01	2.55	LL	-4	-0.9	38	1000	994	451	2	344	4	210	0	0.99	1.00	0	-0.69	0.08	0.21	
3	high	low	high	5.81	0.03	LL	-4	-0.9	38	982	929	497	32	435	33	176	3	0.93	1.00	0	-0.59	0.08	0.31	
4	high	high	high	5.81	2.55	LL	-4	-0.9	38	116	21	548	408	530	375	26	4	0.02	0.90	0	-0.36	1.90%	0.07	0.54
5	low	low	low	0.01	0.03	UR	4	0.9	38	422	0	1000	999	243	0	240	0	1.00	1.00	0	0.78	0.08	0.12	
6	low	high	low	0.01	2.55	UR	4	0.9	38	339	1	1000	998	271	1	207	0	1.00	1.00	0	0.77	0.10	0.13	
7	high	low	high	5.81	0.03	UR	4	0.9	38	262	1	1000	994	318	3	154	0	0.94	1.00	0	0.77	0.11	0.13	
8	high	high	high	5.81	2.55	UR	4	0.9	38	42	3	936	826	399	120	43	1	0.83	0.95	0	0.76	0.95	0.17	0.14
9	low	low	low	0.01	0.03	LL	-4	-0.9	20	980	944	286	24	174	12	146	9	0.94	1.00	0	-0.69	0.11	0.21	
10	low	low	low	0.01	0.03	LL	-4	-0.9	100	1000	1000	520	0	380	0	382	0	1.00	1.00	0	-0.84	0.03	0.06	
11	high	high	high	5.81	2.55	LL	-4	-0.9	20	90	41	521	421	472	380	17	2	0.04	0.85	0	-0.44	0.05	0.44	
12	high	high	high	5.81	2.55	LL	-4	-0.9	100	173	39	610	412	571	368	24	4	0.04	0.97	0	-0.23	0.04	0.67	
13	low	low	low	0.01	0.03	LL	-4	-0.5	38	910	799	397	62	363	66	297	46	0.79	0.94	0	-0.47	0.09	0.47	
14	low	low	low	0.01	0.03	LL	-1	-0.9	38	1000	1000	403	0	325	0	203	0	1.00	1.00	0	-0.85	0.06	0.05	
15	low	low	low	0.01	0.03	LL	-4	-0.3	38	665	456	389	175	361	156	314	126	0.46	0.75	0	-0.40	0.08	0.10	
16	high	high	high	5.81	2.55	LL	-4	-0.3	38	44	6	542	414	513	378	31	5	0.01	0.00	0	NA	NA	NA	NA
17	low	low	low	0.01	0.03	UR	4	0.9	38	385	0	999	999	228	0	221	1	1.00	1.00	0	0.78	0.08	0.12	
18	high	high	high	5.81	2.55	UR	4	0.9	38	21	1	937	833	404	90	29	0	0.853	0.95	0	0.76	0.95	0.17	0.14
19	low	low	low	0.01	0.03	LL	-4	-0.9	38	1000	997	416	0	264	0	235	0	1.00	1.00	0	-0.77	0.00	0.13	
20	high	high	high	5.81	2.55	LL	-4	-0.9	38	118	32	345	402	524	390	22	3	0.03	0.84	0	-0.35	2.70%	0.06	0.55

## Chapter 3

### **Pervasive declines in monkfish (*Lophius americanus*) size structure throughout the northwest Atlantic**

Charbonneau, J. A., Keith, D. M., MacNeil, M. A., Sameoto, J. A. and Hutchings, J. A. (2020). Pervasive declines in monkfish (*Lophius americanus*) size structure throughout the northwest Atlantic. *Fisheries Research*, 230, 105633.

#### **3.1 Introduction**

The population dynamics of many present-day marine fish stocks have been influenced by a complex history of exploitation and environmental change [74]. Shifts in size structure have been described for many stocks [55, 73, 49], with long-term patterns of fishing and changing environmental conditions identified as possible mechanisms for observed trends [7, 11]. The consequences of a truncation in size are potentially profound, including altered interspecific interactions [10], compensatory population dynamics [57] and responses to environmental variability [4]. In addition to reduced quality and quantity of offspring [47] and availability to fisheries. Although the extent of these changes remain uncertain, generally stock dynamics are expected to shift towards early maturation and shorter lifespans than former generations [62, 36]. These changes will have consequences for stock productivity and population viability [48], highlighting the importance of understanding the drivers responsible.

Long-term decreases in size have been reported for northwest Atlantic monkfish (*Lophius americanus*) [8, 81], a demersal anglerfish whose distribution broadly spans the north Atlantic, extending from Cape Chidley, Labrador to North Carolina in the United States [88, 82]. However, a comprehensive understanding of the magnitude of this size decrease and the drivers behind this change is lacking. The northern component of the stock is separated by a trans-national management boundary, making monkfish an ideal species in which to study long-term spatiotemporal patterns of demography across areas with marked differences in fishing effort and management

strategies. The Canada-US border straddles the uppermost third of Georges Bank, north of the Gulf of Maine [34]. While no directed fishery for monkfish exists in the Maritimes region of Canada, they are commonly caught as bycatch by both mobile and fixed gear fleets, and can be landed in most groundfish and scallop fishing areas [17]. Conversely, a lucrative fishery exists in the US; developed in the 1980s, it was the highest valued finfish in the northeastern states in the mid-1990s [82].

Monkfish occur in waters of 0-24°C [93] at depths of 70-100 m, however they have been found in excess of 800 m [30]. As ambush predators, they settle into sandy substrates, extending their illicium to attract prey [93]. Although this behavioural strategy limits their mobility, they have been found to undertake seasonal migrations, thought to be linked to temperature, spawning, and food availability among juveniles and adult life stages [26, 84, 82]. As generalists, they consume a wide range of prey, mainly consisting of fish and invertebrates; stomach composition studies have revealed that they may consume prey as large as themselves [84, 91]. Mature monkfish have been observed to reach maximal sizes of 85 cm (males) and 138 cm (females) although considerable uncertainty surrounds their life-history traits [81].

The status of monkfish in the Canadian Maritimes was last assessed nearly two decades ago [8] at which time it was indicated that the proportion of large fish (>60 cm) had declined relative to that of the 1990s. A similar truncation in size was reported in the US, where notable decreases in survey-based lengths were first evident in the 1980s and continued to be observed from 1990 onwards [80, 81]. Subsequent assessments have yet to be scheduled in either country. Here, we quantify temporal changes in the length composition of monkfish, using 55 years of stratified groundfish and scallop survey data from the Department of Fisheries and Oceans (DFO) of Canada and the Northeast Fisheries Science Center (NEFSC) in the US. We apply a linear mixed effects model to examine environmental (e.g. temperature, depth, surveyed area) and anthropogenic (e.g. survey gear, management agency) mechanisms underlying shifts in size structure.

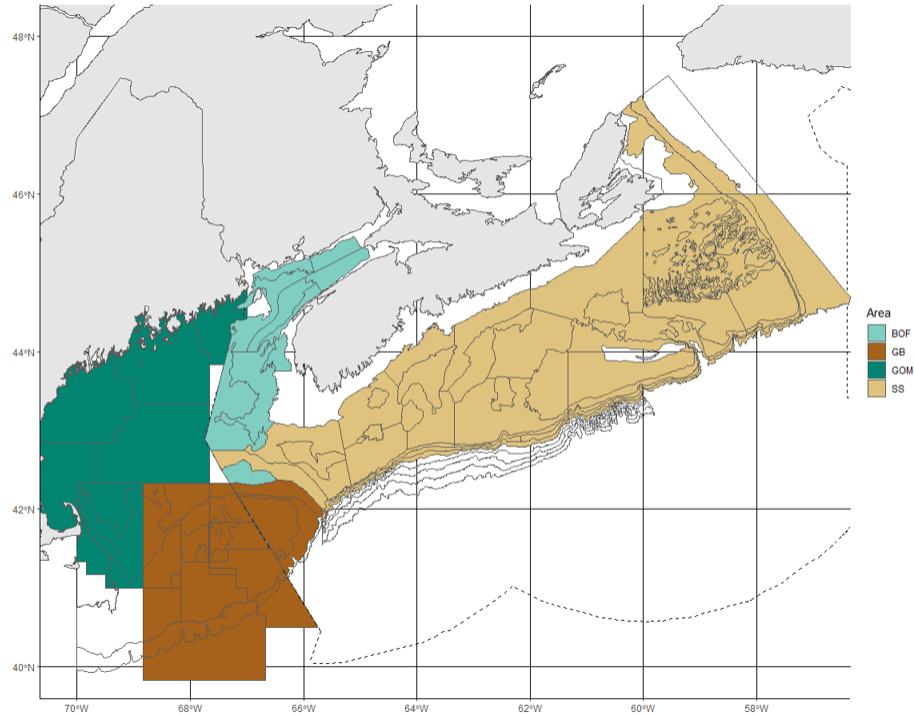


Figure 4: Map of study area. Shaded areas represent the four areas broadly encompassed in the study: the Scotian Shelf (SS) and the Bay of Fundy (BOF), the Gulf of Maine (GOM), and Georges Bank (GB). The dashed line represents the Canadian EEZ. NEFSC statistical areas and DFO survey strata are included for illustrative purposes.

## 3.2 Methods

### 3.2.1 Study area

The northwest Atlantic is divided by the International Court of Justice Hague Line, a management boundary delimiting the Canadian and American jurisdiction of international waters. This border transects the uppermost third of Georges Bank north of the Gulf of Maine, resulting in transboundary fish stocks. The region examined in the present study broadly encompasses four areas: the Scotian Shelf and the Bay of Fundy, the Gulf of Maine, and Georges Bank. These areas were further divided into 70 locations sampled by the research surveys undertaken by both countries (Figure 4).

### **3.2.2 Data sources**

Individual length frequencies (cm) of monkfish were obtained from multiple research surveys from Canada and the United States spanning the time period of 1963 to 2018 (Table 3). Additional data collected on the surveys and included in this analysis were depth, bottom temperature, sampling area, survey season, and gear type.

#### **3.2.2.1 DFO survey**

The time-series for the Canadian Maritimes research vessel survey began in 1970, which coincides with the implementation of the International Commission for the Northwest Atlantic Fisheries (ICNAF) protocol (later to become the Northwest Atlantic Fisheries Organization (NAFO), adopted by both countries [21]. The survey operates primarily in the summer (July - early October) on the Scotian Shelf and in the Bay of Fundy [25]. This region was formerly surveyed in the fall, a practice which was discontinued in 1984 [25]. A spring survey for Georges Bank began in 1986, conducted yearly in February through March [32]. Each survey follows a stratified random sampling design, however their strata, geographical extent, and depth range varies, with the total depth covered by all surveys combined ranging from approximately 11 to 395 m (Table 3; [90]).

Surveys were mainly conducted using the Atlantic Western IIA trawls (hereafter Western IIA trawl) at depths ranging from approximately 30 to 400 m [31]. Detailed biological sampling (e.g. related to age, growth, maturity and stomach composition) commenced in the 1990s [21]. Several vessel changes have been made over the course of nearly 50 years of sampling. Key research vessels include the A.T Cameron, in service from 1970 to 1981, replaced briefly by the Lady Hammond in 1982. The Alfred Needler has been the primary vessel since 1983, occasionally superseded by the Teleost from 1996 onwards, in years when the former was in need of servicing [25].

#### **3.2.2.2 NEFSC survey**

The NEFSC offshore bottom trawl groundfish surveys have been operating in the fall and spring since 1963 and 1968, respectively [82]. While these two seasons comprise

the majority of data used to conduct stock assessments, additional surveys have been implemented. Namely, the summer scallop dredge survey since 1984 and the winter flatfish bottom trawl survey (not included in the analysis) since 1992 (Table 3; [82]).

As is the case with Canada, a stratified random sampling design was implemented. The Albatross, a stern trawler, was used as the principal sampling vessel for the groundfish surveys from 1992 to 2008, later replaced by the Henry Bigelow which has been in commission from 2009 onward. The main gear type employed are Yankee trawls for the groundfish surveys and dredges for the scallop surveys. See Tables 1 and 2 for additional specifications regarding gear included in the analysis.

### **3.2.2.3 Data used for the analysis**

The analysis consisted of data from the research vessel groundfish bottom trawl surveys and the United States scallop survey, combining data from DFO and NEFSC. Survey tows were restricted to those ranked as ‘good’ or ‘representative’. Additional details regarding the duration of the survey, the number of observations and the geographic coverage can be found in Tables 3 and 4. Gear types that did not differ significantly in size-selectivity (as determined by ANOVAs) were grouped into the following categories: Yankee trawl, modified Yankee trawl, and scallop dredge for the US, and Western IIA trawl for Canada (for additional details see Table 3). Sampling gear used inconsistently over time and/or with fewer than 500 observations were removed. The area in which the surveys overlapped (i.e. Canadian sampling sites on the American side of the Hague Line and vice versa) was removed as these 11 sampling sites confounded the analysis. A subset of overlapping surveys from the DFO Western IIA trawls and NEFSC Yankee trawls, constrained to Georges Bank and controlling for year and seasonality, was subsequently examined to evaluate the comparability between observed length frequencies between Canadian and American Groundfish bottom trawl surveys.

The data were explored prior to the analysis to determine the spread and distribution, to discern any relationships between variables, to distinguish if data transformation was necessary and to identify outliers. Bottom temperature and depth were centered in addition to year, which was centered at 1981, at which time most gear types (with the exception of scallop dredge) were represented. Baseline levels of

categorical and numerical covariates were adjusted in ascending order, as a function of the number of observations.

### 3.2.3 Statistical analyses

#### 3.2.3.1 All subareas

Spatiotemporal changes in the length composition of monkfish were investigated using a linear mixed effects modelling framework. The fixed effects of different model variations were tested, using the Akaike's Information Criterion (AIC) to determine the relative support for each model. The best model was favoured over other configurations with  $\Delta$  AIC 32 lower than the next ranked model (Table 5).

$$\begin{aligned}
 L_{is} & N(mu_{is}, \sigma^2) \\
 \varepsilon_i & N(0, \sigma^2) \\
 mu_{is} & = Season_{is} + Bottomtemp_{is} + Depth_{is} + Year * Surveygear_{is} + Year + Year_s \\
 Area_s & N(0, \sigma_{Area}^2) \\
 Year_s & N(0, \sigma_{Year}^2)
 \end{aligned}
 \tag{1}$$

where the response variable  $L_{is}$ , is the length (cm) of individual  $i=1, \dots, 18929$  in area  $s=1, \dots, 70$ .  $Year_s$  is the random slope of Year (1963-2018) for each area and  $Area_s$  the random intercept of area which are assumed to be normally distributed with a mean of 0 and variance  $\sigma^2$ . The fixed effects included bottom temperature (°C) and depth (m) which were centered, with survey gear (Yankee trawl, Modified Yankee trawl, Western IIA trawl, scallop dredge) and season (spring, summer, fall) as categorical factors. Year was included as an interaction with survey gear. Estimates of fit were obtained using restricted maximum likelihood (REML) (Table SB1) and 95 % confidence intervals were calculated by multiplying standard error by 1.96. Model assumptions were examined by performing diagnostics (e.g. verifying linearity of variables, independence and normality of residuals and partial residuals, independence and linearity of variables).

### 3.2.3.2 Canada-US bottom trawl survey comparison

A second analysis was performed, using a subset of data for Georges Bank, to compare observed monkfish average lengths between Canadian and US bottom trawl surveys. The data were restricted to the principal surveying gear in each respective country (Western IIA trawl for DFO and Yankee trawl for NEFSC) during the spring from 1996 to 2018, at which time the surveys overlapped (Table 3). Controlling for location, seasonality, and year allowed for the detection of discrepancies in observed lengths between the principal groundfish surveys in either country to assess their comparability. The parameters were selected based on the previous model (equation 1) which was favoured over the second-best model by a  $\Delta$  AIC score of 1.44 (Tables SB2 and SB3):

$$\begin{aligned} L_i & \sim N(\mu_i, \sigma^2) \\ \varepsilon_i & \sim N(0, \sigma^2) \\ \mu_i & = Year_i + Bottomtemp_i + Depth_i + Surveygear_i \end{aligned} \tag{2}$$

where the response variable  $L_i$ , is the length (cm) of individual in  $i=1, \dots, 1189$ , in  $Year$  (1996-2018), centered at 2007 to represent the median of the time-series. The fixed effects included bottom temperature ( $^{\circ}\text{C}$ ) and depth (m), which were centered and survey gear (i.e. Western IIA trawl or Yankee trawl). Model assumptions were verified (see “all subareas” analysis, equation 1), model selection included in Table SB3.

## 3.3 Results

### 3.3.1 Temporal patterns in size structure

Data were available to investigate changes in size structure of monkfish over the course of 55 years (1963-2018). Widespread decreases in the average length of fish were evident over the course of the time-series in both countries, with an overall



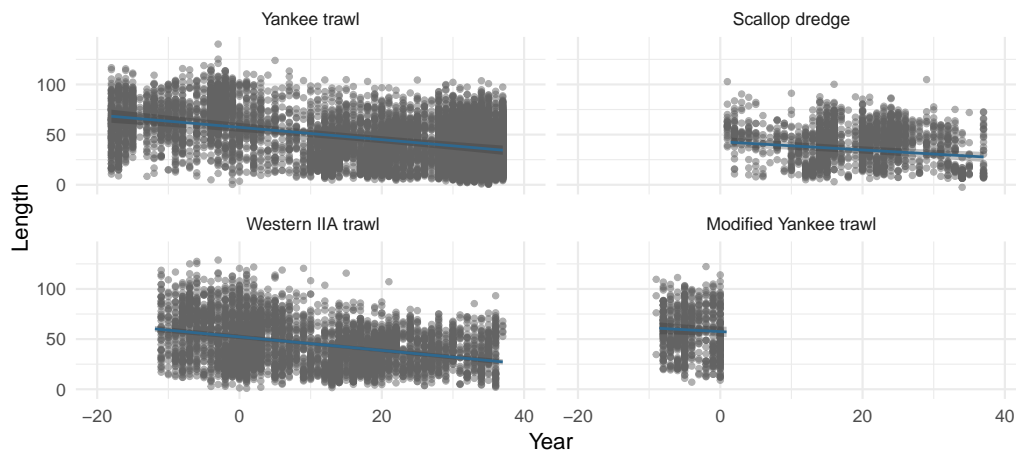


Figure 5: Partial residuals of modelled monkfish length frequencies (equation 1) for each respective gear type (US: Yankee trawl, Modified Yankee trawl, scallop dredge; Canada: Western IIA trawl) with slopes and 95 % confidence intervals superimposed. Note model is centered, where year 0 is 1981.

decline of 48 % in size occurring at a rate of 0.61 cm.year<sup>-1</sup> ( $\pm 0.16$  cm.year<sup>-1</sup>, 95 % C.I.) (Figure 5, Table SB1). An average-sized monkfish in the studied area was 71.00 cm in 1963, diminishing to 37.19 cm in 2018; representing a 33.81 cm decline (Table SB1). Although differences in length were observed between gear types, the overall trend of decreasing size was evident across gears.

### 3.3.2 Spatial patterns in size structure

Best linear unbiased predictions (BLUPs) were used to discern spatial patterns in the random effect of area ( $n = 70$ ) generated by the linear mixed model. The trends documented above were inspected visually by spatially plotting the random intercepts and slopes. Fish were larger on average in the Bay of Fundy and in certain sampling locations in the US, as represented by the higher intercept values (Figure 6). The steepest declines occurred along certain areas of the Scotian Shelf, as illustrated by the modelled slopes (Figure 6). The rate of decline was lowest (with increases in some cases) on Georges Bank and several strata along the Scotian Shelf.

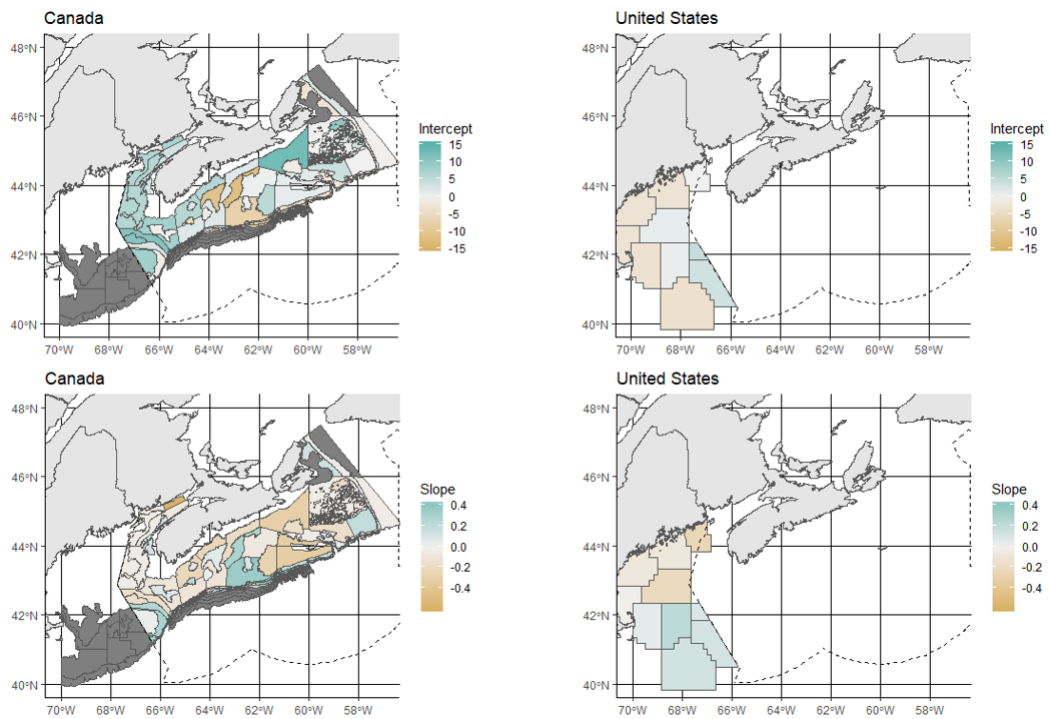


Figure 6: Map of study area. Shaded areas represent BLUPs (standard deviations from the Canadian (DFO) and US mean (NEFSC))  $n=70$ , where positive and negative intercepts and slopes are represented and shaded according to scale and areas with values of 0 are shaded grey. The dashed line represents the Canadian EEZ. NEFSC statistical areas and DFO survey strata are included for illustrative purposes.

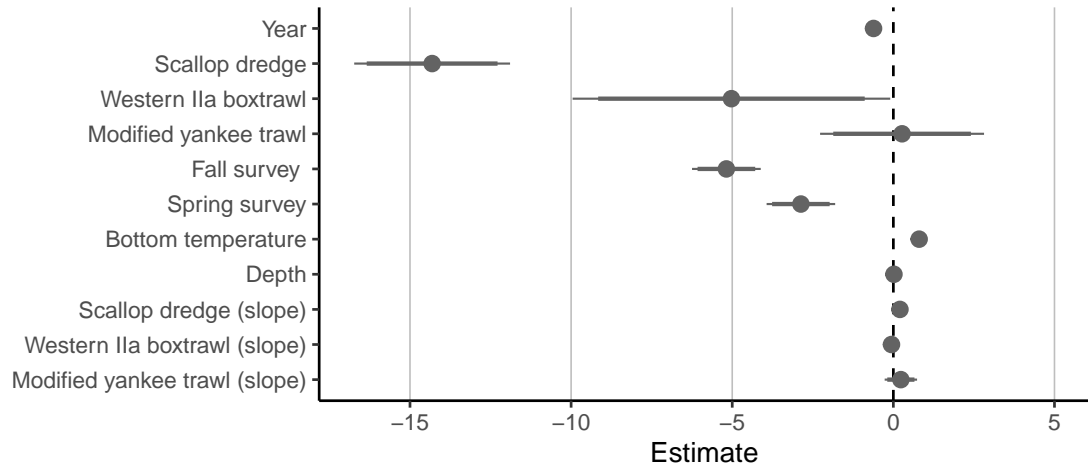


Figure 7: Effect size plot from a linear mixed model analysis of monkfish length frequencies  $n=20,290$  across Canada and the United States (US: Yankee trawl, Modified Yankee trawl, Scallop dredge; Canada: Western IIA trawl). Circles represent the estimates, thick and thin bars represent 90 % and 95 % uncertainty intervals, respectively. Positive values correspond to increased length relative to the baselines (gear type: Yankee trawl, season: summer). Year centered at 1981.

### 3.3.3 Other factors affecting size

#### 3.3.3.1 Gear

No differences were found between the fish sampled by Yankee trawls and modified Yankee trawls (Table SB1). Scallop dredges sampled smaller monkfish than other gear types, sampling 14.31 cm and 9.29 cm ( $\pm 2.42$  cm) smaller fish than Yankee trawls and Western IIA trawls, respectively (Figure 7, Table SB1). However, the temporal rate of decrease for this gear was less steep by 0.20 cm.year<sup>-1</sup> when compared with the US Yankee trawl and by 0.26 cm.year<sup>-1</sup> ( $\pm 0.10$  cm) than the Canadian Western IIA trawl.

Significant differences in average length (i.e. intercepts) were observed between the US and Canada groundfish bottom trawl surveys in the overall model analysis, with the average monkfish sampled by Yankee trawls 5.02 cm ( $\pm 4.93$  cm) larger than those caught in Western IIA trawls (Figure 7, Table SB1). Subsequent analyses which controlled for location, season, and year, indicated that the US Yankee trawl caught fish that were 6.24 cm ( $\pm 3.67$  cm) larger on average than those sampled by the Canadian Western IIA trawl (Tables SB2 and SB3, Figure SB1).

### **3.3.3.2 Season, temperature and depth**

Length differed significantly by season, with fish observed in summer 2.86 cm and 5.18 cm ( $\pm 1.06$  cm) larger on average than those in the spring and fall, respectively (Figure 7, Table SB1). The average length of individuals increased significantly with bottom temperature, at a rate of 0.80 cm. $^{\circ}$ C-1 ( $\pm 0.15$  cm. $^{\circ}$ C-1) (Figure 7, Table SB1). The effect of depth on monkfish length was negligible, with an increase of 0.018 cm.m-1 ( $\pm 0.007$  cm.m-1) (Figure 7, Table SB1). It must be noted that the US survey samples a wider range of depths (11-395 m) than Canada (13-209.5 m).

## **3.4 Discussion**

The present study documents changes in the length composition of northwest Atlantic monkfish, a transboundary stock experiencing considerable differences in resource use and management regimes across two jurisdictions. Substantial decreases in average monkfish length were evident in both Canada and the United States over the span of 55 years (1963-2018), with the average fish 33.81 cm smaller than those sampled at the beginning of the time-series, representing a 48 % decrease in historic body length. The rate of decrease did not differ significantly between countries, despite the existence of an ongoing and gainful fishery in the US, which is presumed to exhibit higher levels of fishing mortality than in the Canadian Maritimes, for which a targeted fishery is absent [8, 81].

### **3.4.1 Inter-country discrepancies in size-selectivity**

Monkfish sampled by the American Yankee trawls were 5 cm larger on average than those sampled by the Canadian Western IIA trawls (Table SB1, Figures 4 and 5), however the rate of decrease was similar in both countries at approximately 0.61 cm.year-1 ( $\pm 0.16$  cm). This discrepancy was further examined in a second analysis restricted to a subset of data on Georges Bank and controlling for area, season, and year, to determine if the observed differences in size represented true spatial patterns or were simply an artifact of the sampling gear. The analysis revealed incongruencies between the observed size in neighbouring countries surveys, with the principal American survey (Yankee trawl) sampling fish 6 cm larger on average than

those caught by the Canadian survey (Western IIA trawl; Tables SB2 and SB3, Figure SB1), with no significant differences in the rate of decrease. This disparity may be attributed to structural differences between the principal sampling equipment utilized in either country. Western IIA trawls are equipped with larger rollers than Yankee trawls, potentially making them less suitable to sample monkfish, which settle into the substrate [18]. These differences call into question the systematization of the NAFO protocol for standardizing stratified random bottom trawl surveys employed by both countries. Further, the implications of this difference should be considered when combining fish length data from multiple surveys.

Although trawls are the standardized gear used for traditional groundfish surveys, there has been some debate surrounding the accuracy of the gear used insofar as collecting representative samples of monkfish [56, 90]. It has been suggested that scallop dredges are better suited to access these benthic fish [90]. We find that the dredges sample significantly smaller monkfish than the primary American (Yankee) and Canadian (Western IIA) trawls, by an average of 14.31 cm and 9.29 cm ( $\pm$  0.10 cm), respectively. Selectivity differs between gear types, which may explain the discrepancy in size between the dredges and other survey gear. To complicate matters, Richards et al. (2008) [82] suggests that the wide depth distribution of monkfish could render a large proportion of the population inaccessible to survey gear. Temporal changes in vessels also present a challenge as the resulting differences in size and towing power lend to inconsistent catchabilities across ships [81].

### **3.4.2 Drivers underlying the observed trends**

Fisheries are size-selective in nature and prolonged, non-random patterns of mortality have the potential to influence the size structure of a stock, which can lead to reductions in mean age and size at maturity [77, 62, 96]. Older and larger fish are often preferentially selected by fishing gear, increasing the contribution of small fish to the population [89], which over time is thought to truncate the age and size structure of exploited stocks. While this phenomenon is supported in experimental studies that have suggested that fishing can generate genetic responses in fished populations [43], disentangling genetic effects from plastic responses remains a challenge for wild stocks [77, 58]. The concept of fishery-induced evolution is thought to have a particularly

strong influence on traits related to age and size at maturity [60, 42]. Monkfish are almost exclusively caught in multispecies fisheries, making them vulnerable to multiple gear types, notably bottom trawls and scallop dredges [2]. The size-selectivity of these types of gear could have considerable demographic consequences for the stock, given the larger sizes and longer lifespan attained by females relative to males, which could generate preferential gear-selection towards larger reproductive fish. While long-term sex-specific data were not available, Johnson et al. (2008) [56] found that monkfish >70 cm were generally mature females, a size class infrequently observed in the survey in recent years.

The influence of fishing mortality on temporal patterns of size structure could not be directly examined because of non-existent or incomplete records of fishery removals. The first documented removals in Canada are bycatch that can be traced as far as the 1960s; however, the reliability of these data remains uncertain [30]. The paucity of monkfish landings data can be attributed to limited markets for the species prior to 1986, leading to underreporting and discarding [30]. Subsequently, higher market prices in the 1990s led to an increase in commercial catch [30]. Landings in the Maritimes have since been variable, thought to be attributed to changes in the market as well as economic disincentives [8].

Monkfish landings began increasing in the US in the mid 1970s, before which they were considered ‘trash’ fish and were repurposed as fish meal. Armstrong et al. (1992) [3] attribute this development to the deterioration of other traditional groundfish species. The stock is divided into a northern and southern management component, which are thought to be genetically homogeneous [24]. In 2003, both components were considered to be overfished with fishing mortality generally decreasing thereafter [80].

Quantifying effort in either country remains a challenge due to the reliance of multispecies fisheries and frequent incidental bycatch [2, 17]. The Canadian scallop fisheries have a high incidence of monkfish bycatch [40, 86]. However, the rate of decline in monkfish length was lower across Georges Bank and the Bay of Fundy – areas fished heavily and consistently for scallop. This, taken with the uniform rate of decrease across areas characterized by drastically different resource use, suggests that other biotic and abiotic factors (e.g. bottom temperature, depth, species interactions) may be influencing the underlying temporal trends in monkfish size structure.

Bottom temperature significantly impacted the size of monkfish in the model, as the average length of individuals increased at a rate of 0.80 cm. $^{\circ}$ C $^{-1}$  ( $\pm$  0.15 cm. $^{\circ}$ C $^{-1}$ ). While temperature has commonly been linked to physiological response in many fish species, a decreased size has been suggested in response to reductions in oxygen solubility and increased anabolic oxygen demand that accompany warming waters [7]. Evidence for this phenomenon has been well documented for several species such as haddock (*Melanogrammus aeglefinus*) [6], European plaice (*Pleuronectes platessa*) [98] and Atlantic herring (*Clupea harengus*) [15]. This is relevant in areas such as the northwest Atlantic, where thermal regimes are shifting with warming [9]. The opposing response exhibited by monkfish could be related to their optimal thermal range; although much is left to be understood regarding their life-history, it is possible that current temperatures are not representative of their thermal maxima. It is also possible that this relationship is affected by temperature-driven seasonal movements [90].

The incidence of smaller monkfish in fall and spring compared to summer could be related to spawning, which begins in spring in the south continuing into early fall in the north [82], conceivably increasing the proportion of smaller fish. A study by Siemann et al. (2018) [90], using data from scallop dredge surveys, found seasonal differences in bottom temperatures to influence monkfish distribution on Georges Bank. They found monkfish to be most abundant and more widely distributed in summer and early fall, compared to winter months, when they were concentrated in deep water and bank edges [90]. Similar temperature-driven movements were evidenced in a related species of anglerfish (*Lophius piscatorius*), where increased abundance and range expansion in the mid-1980s were linked to increases in ambient bottom temperatures [92]. This implies that temperature could have a similar effect on northwestern Atlantic monkfish which share much of their biology with their northeastern counterpart [38]. Temperature-driven changes in distribution have been documented for several fish species on the northeast continental shelf [67]. However, Richards (2016) [81] did not find any indication of temporal range shifts in the most recent operational monkfish assessment.

A multitude of factors can act either independently or concurrently to govern body size in fish. For instance, density dependence and compensatory dynamics can

influence individual size [57]. Svedäng and Hornborg (2014) [96] found size-selective fishing practices to be the cause of size truncation in Western Baltic cod (*Gadus morhua*), with a 30 % decrease in mean size from 1991 to 2016. The increases in juvenile fish that followed strengthened density-dependent dynamics, lowered individual growth, and increased competition. Although the data are not available to track monkfish cohorts through time in Canada and the United States, the most recent US operational assessment highlighted the need to better understand density-dependent growth under the recommended areas of research [81].

### **3.4.3 Implications of decreasing body size**

The implications of decreasing body size on reproduction are numerous. Relative fecundity is said to increase as a function of length in marine fish, with the quality and quantity of eggs increasing with the size of reproductive-aged females in some species [11]. Larger fish are able to allocate more of their energy to producing eggs and support a greater volume than their smaller counterparts [11]. This hypothesis has been supported by studies of bocaccio rockfish (*Sebastes paucispinis*), for which a doubling in length corresponded to a near 10-fold increase in fecundity [12]. Similarly, Marshall et al. (2006) [64] examined a 56 year time-series of Northeast Arctic Atlantic cod, finding relative fecundity to have a positive correlation with mean length. There is considerable merit in exploring trends in monkfish weight, although spatiotemporal inconsistencies in individual measurements between data collected by the DFO and the NEFSC left this question beyond the scope of the current research. Changes in demography are also likely to impact the diverse inter-specific interactions between monkfish and their associated predator and prey species. In addition, the increased yield of smaller fish to fisheries will necessarily present economic ramifications, especially in the US, where there is a lucrative commercial fishery.

## **3.5 Conclusions**

The northern monkfish stock in the northwest Atlantic straddles two countries, with considerable differences in fishing and management regimes. While survey data are collected on this species, differences in sampling protocols make transboundary differences in data type and quality difficult to resolve. For example, certain measurements



are inconsistent in space and time (e.g. individual weight, fishing mortality) and aspects of survey methodology (e.g. vessels, gear, surveyed area) and data collection (e.g. binning) were subject to change over time. Challenges arise in the Maritimes region of Canada, where the lack of a directed fishery has limited the frequency of stock assessments and the collection of biological data. An initial study examining bycatch indicated that the proportion of monkfish caught incidentally was substantial [40], however subsequent detailed evaluations of bycatch have yet to be undertaken.

Comparatively, more information is available for the US, however there is a need for improvement regarding the characterization of acceptable biological catch (ABC) control rules and the development of an accurate ageing protocol [81]. Updated assessments, an improved understanding of the ecological role of monkfish, and the development of management frameworks aimed at rebuilding the lost size structure are warranted in both countries. Understanding the causal mechanisms responsible for widespread decreases in size structure documented in the present research, and the consequences associated with these changes to population viability and economic returns, will be necessary to ensure the sustainability of the resource.

Table 3: Specifications and spatiotemporal coverage of gear used in the analysis. GOM=Gulf of Maine, GB=Georges Bank, BOF=Bay of Fundy and SS=Scotian Shelf. Nb: Canada and the United States divide survey seasons differently. In the analysis the seasons are divided such that: fall=September-December, spring=January-May, summer=June-August.

<b>Gear ID</b>	<b>Type</b>	<b>Year</b>	<b>Country</b>	<b>Season</b>	<b>Coverage</b>	<b>Bottom temperature (°C)</b>	<b>Depth (m)</b>	<b>Observations</b>
11	Yankee trawl	1963-2008	United States	Fall, Spring, Summer	GOM, GB, BOF	0.00-16.69	11-395	5049
10	Yankee trawl	2009-2018	United States	Fall, Spring, Summer	GOM, GB, BOF	3.34-17.22	22-373	6503
17	Yankee trawl	1992-2002, 2004	United States	Spring	GB	3.70-19.98	64-215	483
41	Modified Yankee trawl	1973-1981	United States	Spring, Summer	GOM, GB, BOF	2.50-13.40	25-388	754
3	Western IIA trawl	1970-1981	Canada	Summer	BOF, SS	0.48-12.11	17-205	972
9	Western IIA trawl	1978-2018	Canada	Fall, Summer	GB, BOF, SS	0.30-15.45	13-206	4940
82	Scallop dredge	1984-2003	United States	Fall, Summer	GOM, GB	4.06-17.80	21-131	4830
85	Scallop dredge	2008-2015	United States	Spring, Summer	GOM, GB	4.53-14.57	45-135	862
86	Scallop dredge	2008-2018	United States	Spring, Summer	GOM, GB	4.47-13.10	33-134	562
83	Scallop dredge	2004-2007	United States	Summer	GOM	4.22-11.47	30-118	268

Table 4: Spatiotemporal coverage of surveys in Canada and the United States. Where GOM=Gulf of Maine, GB=Georges Bank, BOF=Bay of Fundy, SS=Scotian Shelf and observations are individual length frequencies.

<b>Subarea</b>	<b>Country</b>	<b>Year</b>	<b>Observations</b>
GOM	United States	1963-2018	11,637
GB	United States	1963-2018	7,674
SS	Canada	1970-2018	5,227
BOF	Canada	1970-2018	538
GB	Canada	1986-2018	147

Table 5: Relative support for linear mixed effects models tested in equation 1. Monkfish length (cm) as a function of different fixed effect predictors with a random slope of year and random intercept of area, where df represents degrees of freedom, LogLik is the log likelihood,  $\Delta$  AIC is the relative difference in Akaike Information Criterion and  $w_i$  are the Akaike weights

<b>Model</b>	<b>df</b>	<b>LogLik</b>	<b><math>\Delta</math>AIC</b>	<b><math>w_i</math></b>
length~(year area) + year*surveygear + season + bottomtemp + depth	16	-14683.04	0	9.99e-01
length~(year area) + year*surveygear + season + bottomtemp	15	-14700.29	32.49	8.80e-08
length~(year area) + year*surveygear + season + depth	15	-14742.73	117.37	3.27e-26
length~(year area) + year + surveygear+ season+ bottomtemp	12	-14700.46	26.83	1.49e-06

## Chapter 4

### Conclusion

My thesis involved analyses of large-scale temporal shifts in the age and size structure of commercially exploited fishes. In Chapter 2, examination of 43 stocks allowed for the evaluation of sensitivity and response time in age structure following historic levels of fishing mortality. Significant responses were exhibited in 88 %, varying widely between stocks, likely a result of unique life histories, exploitation, and management. Chapter 3 investigated changes in northwest Atlantic monkfish size structure, finding a 48 % reduction in average body length over the 55-year period. Surprisingly, this decrease was more pronounced in Canada compared to the United States, where the former lacks a commercial fishery. This suggests that other factors such as bycatch, gear, season, temperature, or depth are likely responsible for the associated changes. Both of these projects apply quantitative ecological methods to evaluate long-term trends of biologically important traits related to age or size with the common thread of investigating the possible causes and consequences for the resulting shifts. These findings contribute to the growing body of work aimed at studying how anthropogenic and environmental factors interact to influence the dynamics of targeted fish species and highlights the importance of better understanding intraspecific trait variation, to strengthen our capacity to predict future changes and manage accordingly.

## Bibliography

- [1] M.S Allen and W.E Pine. Detecting Fish Population Responses to a Minimum Length Limit: Effects of Variable Recruitment and Duration of Evaluation. *North American Journal of Fisheries Management*, 20(3):672–682, 2000.
- [2] Gregory Ardini, Douglas Christel, Patricia Clay, Correia Steven, Jason Did-den, Jerome Hermsen, Fiona Hogan, F Palmer, M Pentony, K Richardson, and A Richards. Monkfish fishery management plan framework adjustment 9, north-east multispecies fishery management plan framework adjustment 54: incorporating stock assessment and fishery evaluation (safe) report for the 2013 fishing year and the environmental assessment. Technical report, New England Fishery Management Council, 2016.
- [3] Michael P. Armstrong, John A. Musick, and James A. Colvocoresses. Age, growth and reproduction of the goosefish *Lophius americanus* (Pices:Lophiiformes). *Fishery Bulletin*, 90(2):217–230, 1992.
- [4] A. Audzijonyte, A. Kuparinen, R. Gorton, and E. A. Fulton. Ecological consequences of body size decline in harvested fish species: positive feedback loops in trophic interactions amplify human impact. *Biology Letters*, 9(2):1103–1103, 2013.
- [5] Lewis A.K. Barnett, Trevor A. Branch, R. Anthony Ranasinghe, and Timothy E. Essington. Old-Growth Fishes Become Scarce under Fishing. *Current Biology*, 27(18):2843–2848.e2, 2017.
- [6] A. R. Baudron, C. L. Needle, and C. T. Marshall. Implications of a warming North Sea for the growth of haddock *Melanogrammus aeglefinus*. *Journal of Fish Biology*, 78(7):1874–1889, 2011.
- [7] Alan R. Baudron, Coby L. Needle, Adriaan D. Rijnsdorp, and C. T Marshall. Warming temperatures and smaller body sizes: synchronous changes in growth of North Sea fishes. *Global Change Biology*, 20(4):1023–1031, 2014.
- [8] D Beanlands, R Branton, and R Mohn. The Status of Monkfish in 4VWX5Zc. Canadian Stock Assessment Secretariat 2000/143, Department of Fisheries and Oceans Canada, Dartmouth, Nova Scotia, 2000.
- [9] Igor M. Belkin. Rapid warming of Large Marine Ecosystems. *Progress in Oceanography*, 81(1-4):207–213, 2009.
- [10] Hp Benoît, Dp Swain, Wd Bowen, Ga Breed, Mo Hammill, and V Harvey. Evaluating the potential for grey seal predation to explain elevated natural mortality in

- three fish species in the southern Gulf of St. Lawrence. *Marine Ecology Progress Series*, 442:149–167, 2011.
- [11] S. A. Berkeley, C. Chapman, and S. M. Sogard. Maternal age as a determinant of larval growth and survival in a marine fish, *Sebastes melanops*. *Ecology*, 85(5):1258–1264, 2004.
- [12] Steven A. Berkeley, Mark A. Hixon, Ralph J. Larson, and Milton S. Love. Fisheries Sustainability via Protection of Age Structure and Spatial Distribution of Fish Populations. *Fisheries*, 29(8):23–32, 2004.
- [13] C Birkeland and P Dayton. The importance in fishery management of leaving the big ones. *Trends in Ecology & Evolution*, 20(7):356–358, 2005.
- [14] Gregory L. Britten, Michael Dowd, Lisa Canary, and Boris Worm. Extended fisheries recovery timelines in a changing environment. *Nature Communications*, 8:15325, 2017.
- [15] T Brunel and M Dickey-Collas. Effects of temperature and population density on von Bertalanffy growth parameters in Atlantic herring: a macro-ecological analysis. *Marine Ecology Progress Series*, 405:15–28, 2010.
- [16] Thomas Brunel. Age-structure-dependent recruitment: a meta-analysis applied to Northeast Atlantic fish stocks. *ICES Journal of Marine Science*, 67(9):1921–1930, 2010.
- [17] S. Butler and S. Coffen-Smout. Maritimes Region Fisheries Atlas: Catch Weight Landings Mapping (2010–2014). Technical report 3199, Fisheries and Oceans Canada, Dartmouth, Nova Scotia, 2017.
- [18] P.J.G Carrothers. Scotia-Fundy Groundfish Survey Trawls. Canadian Technical Report of Fisheries and Aquatic Sciences 1609, Department of Fisheries and Oceans Canada, St. Andrews, New Brunswick, 1988.
- [19] Natacha Carvalho, Jordi Guillen, Michael Keatinge, European Commission, Joint Research Centre, and Technical and Economic Committee for Fisheries (STECF) Scientific. *The 2018 annual economic report on the EU fishing fleet (STECF 18-07)*. 2018. OCLC: 1111199132.
- [20] Northeast Fisheries Science Center. 55th Northeast Stock Assessment Workshop (SAW) report. Stock Assessment, 2012.
- [21] E.M.P Chadwick, W Brodie, E Colbourne, D Clark, D Gascon, and T Hurlbut. History of annual multi-species trawl surveys on the Atlantic coast of Canada. *Atlantic Zonal Monitoring Program Bulletin*, 6:25–42, 2007.
- [22] Julie A Charbonneau, David M Keith, and Jeffrey A Hutchings. Trends in the size and age structure of marine fishes. *ICES Journal of Marine Science*, 76(4):938–945, 2019.

- [23] Eric L. Charnov and David Berrigan. Evolution of life history parameters in animals with indeterminate growth, particularly fish. *Evolutionary Ecology*, 5(1):63–68, 1991.
- [24] HM Chikarmane, AM Kuzirian, R Kozlowski, M Kuzirian, and T Lee. Population genetic structure of the goosefish, *Lophius americanus*. *The Biological Bulletin*, 199(2):227–228, 2000.
- [25] R Claytor, D Clark, T McIntyre, H Stone, A Cook, L Harris, J Simon, P Emery, and P Hurley. Review of Surveys Contributing to Groundfish Assessments with Recommendations for an Ecosystem Survey Program in the Maritimes Region. Technical report 3083, Fisheries and Oceans Canada, 2014.
- [26] D.O Conover and S. B Munch. Sustaining Fisheries Yields Over Evolutionary Time Scales. *Science*, 297(5578):94–96, 2002.
- [27] C Costello, BP Kinlan, SE Lester, and SD Gaines. The Economic Value of Rebuilding Fisheries. OECD Food, Agriculture and Fisheries Papers 55, 2012.
- [28] A. J Crean and D. J Marshall. Coping with environmental uncertainty: dynamic bet hedging as a maternal effect. *Philosophical Transactions of the Royal Society B: Biological Sciences*, 364(1520):1087–1096, 2009.
- [29] Chris T Darimont, Stephanie M Carlson, Michael T Kinnison, Paul C Paquet, Thomas E Reimchen, and Christopher C Wilmers. Human predators outpace other agents of trait change in the wild. *PNAS*, 106(3):952–954, 2009.
- [30] DFO. Monkfish on the Scotian Shelf and Northeast Georges Bank (4VWX and 5Zc). Stock Status Report A3-30(2000), Department of Fisheries and Oceans Canada, 2000.
- [31] DFO. 2016 Maritimes Research Vessel Survey Trends on the Scotian Shelf and Bay of Fundy. Canadian Science Advisory Secretariat (CSAS) 2017/004, Fisheries and Oceans Canada, 2016.
- [32] DFO. 2017 Maritimes Winter Research Vessel Survey Trends on Georges Bank. Canadian Science Advisory Secretariat Research Document 2017/035, Fisheries and Oceans Canada, 2017.
- [33] Carlos M. Duarte, Susana Agusti, Edward Barbier, Gregory L. Britten, Juan Carlos Castilla, Jean-Pierre Gattuso, Robinson W. Fulweiler, Terry P. Hughes, Nancy Knowlton, Catherine E. Lovelock, Heike K. Lotze, Milica Predragovic, Elvira Poloczanska, Callum Roberts, and Boris Worm. Rebuilding marine life. *Nature*, 580(7801):39–51, 2020.
- [34] John Alton Duff. The Hague Line in the Gulf of Maine: Impetus or Impediment to Ecosystemic Regime Building? *Ocean and Coastal Law Journal*, 15:285, 2010.



- [35] Katja Enberg, Christian Jørgensen, Erin S. Dunlop, Øystein Varpe, David S. Boukal, Loïc Baulier, Sigrunn Eliassen, and Mikko Heino. Fishing-induced evolution of growth: concepts, mechanisms and the empirical evidence: Fishing-induced evolution of growth. *Marine Ecology*, 33(1):1–25, 2012.
- [36] Katja Enberg, Christian Jørgensen, Erin S Dunlop, Øystein Varpe, David S Boukal, Loïc Baulier, Sigrunn Eliassen, and Mikko Heino. Fishing-induced evolution of growth: concepts, mechanisms and the empirical evidence: Fishing-induced evolution of growth. *Marine Ecology*, 33(1):1–25, 2012.
- [37] FAO. *The State of World Fisheries and Aquaculture 2020*. FAO, Rome, Italy, 2020.
- [38] AC Farina, M Azevedo, J Landa, R Duarte, P Sampedro, G Costas, M A Torres, and L Canas. Lophius in the world: a synthesis on the common features and life strategies. *ICES Journal of Marine Science*, 65(7):1272–1280, 2008.
- [39] R Fisher. *The genetical theory of natural selection*. Oxford, Dover, New York, 1930.
- [40] S Garvaris, KJ Clark, AR Hanke, CF Purchase, and J Gale. Overview of discards from Canadian commercial fisheries in NAFO Divisions 4V, 4W, 4X, 5Y, 5Z for 2002-2006. Technical Report 2873, Fisheries and Oceans Canada, 2010.
- [41] M. Heino, L. Baulier, D. S. Boukal, B. Ernande, F. D. Johnston, F. M. Mollet, H. Pardoe, N. O. Therkildsen, S. Uusi-Heikkilä, A. Vainikka, R. Arlinghaus, D. J. Dankel, E. S. Dunlop, A. M. Eikeset, K. Enberg, G. H. Engelhard, C. Jorgensen, A. T. Laugen, S. Matsumura, S. Nussle, D. Urbach, R. Whitlock, A. D. Rijnsdorp, and U. Dieckmann. Can fisheries-induced evolution shift reference points for fisheries management? *ICES Journal of Marine Science*, 70(4):707–721, 2013.
- [42] M. Heino and U. Dieckmann. Detecting fisheries-induced life-history evolution: an overview of the reaction-norm approach. *Bulletin of Marine Science*, 83(1):26, 2008.
- [43] Mikko Heino, Beatriz Díaz Pauli, and Ulf Dieckmann. Fisheries-Induced Evolution. *Annual Review of Ecology, Evolution, and Systematics*, 46(1):461–480, 2015.
- [44] Mikko Heino and Olav Rune Godø. Estimating reaction norms for age and size at maturation with reconstructed immature size distributions: a new technique illustrated by application to Northeast Arctic cod. *ICES Journal of Marine Science*, 59(3):562–575, 2002.
- [45] Ray Hilborn. Reinterpreting the State of Fisheries and their Management. *Ecosystems*, 10(8):1362–1369, 2007.

- [46] Ray Hilborn, Ricardo Oscar Amoroso, Christopher M. Anderson, Julia K. Baum, Trevor A. Branch, Christopher Costello, Carryn L. de Moor, Abdelmalek Faraj, Daniel Hively, Olaf P. Jensen, Hiroyuki Kurota, L. Richard Little, Pamela Mace, Tim McClanahan, Michael C. Melnychuk, C oil n Minto, Giacomo Chato Osio, Ana M. Parma, Maite Pons, Susana Segurado, Cody S. Szuwalski, Jono R. Wilson, and Yimin Ye. Effective fisheries management instrumental in improving fish stock status. *Proceedings of the National Academy of Sciences*, page 201909726, 2020.
- [47] M. A. Hixon, D. W. Johnson, and S. M. Sogard. BOFFFFs: on the importance of conserving old-growth age structure in fishery populations. *ICES Journal of Marine Science*, 71(8):2171–2185, 2013.
- [48] J. A. Hutchings. Life history consequences of overexploitation to population recovery in Northwest Atlantic cod (*Gadus morhua*). *Canadian Journal of Fisheries and Aquatic Sciences*, 62:824–832, 2005.
- [49] J. A. Hutchings and J. K. Baum. Measuring marine fish biodiversity: temporal changes in abundance, life history and demography. *Philosophical Transactions of the Royal Society B: Biological Sciences*, 360(1454):315–338, 2005.
- [50] Jeffrey A. Hutchings and Anna Kuparinen. Implications of fisheries-induced evolution for population recovery: Refocusing the science and refining its communication. *Fish and Fisheries*, 21:453–464, 2020.
- [51] Jeffrey A. Hutchings and Ransom A. Myers. Effect of Age on the Seasonality of Maturation and Spawning of Atlantic Cod, *Gadus morhua*, in the Northwest Atlantic. *Canadian Journal of Fisheries and Aquatic Sciences*, 50(11):2468–2474, 1993.
- [52] ICES. Report of the Arctic fisheries working group (AFWG). Technical Report ICES CM 2017/ACOM:06, Copenhagen, Denmark, 2017.
- [53] ICES. Report of the working group on Celtic Seas ecoregion (WGCSE). Technical Report ICES CM 2017/ACOM:13, 2017.
- [54] S Jennings. *Marine fisheries ecology*. John Wiley & Sons, Ltd., 2009.
- [55] S Jennings, S Greenstreet, and J Reynolds. Structural change in an exploited fish community: a consequence of differential fishing effects on species with contrasting life histories. *Journal of Animal Ecology*, 68(3):617–627, 1999.
- [56] A. K. Johnson, R. Anne Richards, Daniel W. Cullen, and Sandra J. Sutherland. Growth, reproduction, and feeding of large monkfish, *Lophius americanus*. *ICES Journal of Marine Science*, 65(7):1306–1315, 2008.

- [57] David M. Keith and Jeffrey A. Hutchings. Population dynamics of marine fishes at low abundance. *Canadian Journal of Fisheries and Aquatic Sciences*, 69(7):1150–1163, 2012.
- [58] Anna Kuparinen and Jeffrey A Hutchings. When phenotypes fail to illuminate underlying genetic processes in fish and fisheries science. *ICES Journal of Marine Science*, 2019.
- [59] Anna Kuparinen and Juha Merila. Detecting and managing fisheries-induced evolution. *Trends In Ecology & Evolution*, 22(12):652–659, 2007.
- [60] R Law. Fishing, selection, and phenotypic evolution. *ICES Journal of Marine Science*, 57(3):659–668, 2000.
- [61] R Law. Fisheries-induced evolution: present status and future directions. *Marine Ecology Progress Series*, 335:271–277, 2007.
- [62] Alan Longhurst. Murphy’s law revisited: longevity as a factor in recruitment to fish populations. *Fisheries Research*, 56(2):125–131, 2002.
- [63] A.R Margetts and S.J Holt. The effects of the 1939-1945 war on the English North Sea trawl fisheries. Technical report, 1948.
- [64] C Tara Marshall, Coby L Needle, Anders Thorsen, Olav Sigurd Kjesbu, and Nathalia A Yaragina. Systematic bias in estimates of reproductive potential of an Atlantic cod (*Gadus morhua*) stock: implications for stock–recruit theory and management. *Canadian Journal of Fisheries and Aquatic Sciences*, 63(5):980–994, 2006.
- [65] G. Marteinsdottir and K. Thorarinsson. Improving the stock-recruitment relationship in Icelandic cod (*Gadus morhua*) by including age diversity of spawners. *Canadian Journal of Fisheries and Aquatic Sciences*, 55(6):1372–1377, 1998.
- [66] G Mertz and R A Myers. A simplified formulation for fish production. *Canadian Journal of Fisheries And Aquatic Sciences*, 55(2):478–484, 1998.
- [67] D G Mountain and S A Murawski. Variation in the distribution of fish stocks on the northeast continental shelf in relation to their environment, 1980-1989. In *ICES Journal of Marine Science Symposia*, volume 195, pages 424–432, 1992.
- [68] S. A. Murawski. Rebuilding depleted fish stocks: the good, the bad, and, mostly, the ugly. *ICES Journal of Marine Science*, 67(9):1830–1840, 2010.
- [69] Ransom A. Myers, Jeffrey A. Hutchings, and Nicholas J. Barrowman. Why do fish stocks collapse? The example of cod in Atlantic Canada. *Ecological Applications*, 7(1):91–106, 1997.
- [70] P. Neubauer, O. P. Jensen, J. A. Hutchings, and J. K. Baum. Resilience and Recovery of Overexploited Marine Populations. *Science*, 340(6130):347–349, 2013.

- [71] Larry A Nielsen. The Evolution of Fisheries Management Philosophy. *Marine Fisheries Review*, page 9, 1976.
- [72] NOAA. 2018 Status of U.S. Fisheries Report to Congress. Technical report, NOAA, 2018.
- [73] E.M Olsen, M Heino, G.R Lilly, J.M Morgan, J Brattey, B Ernande, and U Dieckmann. Maturation trends suggestive of rapid evolution preceded the collapse of northern cod. *Nature*, 428(6986):932, 2004.
- [74] D Pauly, V Christensen, S Guenette, TJ Pitcher, UR Sumaila, CJ Walters, R Watson, and D Zeller. Towards sustainability in world fisheries. *Nature*, 418(6898):689–695, 2002.
- [75] Daniel Pauly and Dirk Zeller. Catch reconstructions reveal that global marine fisheries catches are higher than reported and declining. *Nature Communications*, 7(1), 2016.
- [76] G.J. Piet and J.C. Rice. Performance of precautionary reference points in providing management advice on North Sea fish stocks. *ICES Journal of Marine Science*, 61(8):1305–1312, 2004.
- [77] David Policansky. *Fishing as a cause of evolution in fishes*. The Exploitation of Evolving Resources. Springer, Berlin, Heidelberg, 1993.
- [78] J.G Pope and C.T Macer. An evaluation of the stock structure of North Sea cod, haddock, and whiting since 1920, together with a consideration of the impacts of fisheries and predation effects on their biomass and recruitment. *ICES Journal of Marine Science*, 53(6):1157–1169, 1996.
- [79] Wolfgang Nikolaus Probst, Vanessa Stelzenmüller, and Heino Ove Fock. Using cross-correlations to assess the relationship between time-lagged pressure and state indicators: an exemplary analysis of North Sea fish population indicators. *ICES Journal of Marine Science*, 69(4):670–681, 2012.
- [80] A Richards. Status of Fishery Resources off the Northeastern US, 2007.
- [81] A Richards. 2016 Monkfish Operational Assessment. Northeast Fisheries Science Center Reference Document 16-09, National Marine Fisheries Service, Woods Hole, MA, 2016.
- [82] Annee Richards, R., Paul Nitschke, C., and Katherine Sosebee, A. Population biology of monkfish *Lophius americanus*. *ICES Journal of Marine Science*, 65(7):1291–1305, 2008.
- [83] A. D. Rijnsdorp. Fisheries as a large-scale experiment on life-history evolution: disentangling phenotypic and genetic effects in changes in maturation and reproduction of North Sea plaice, *Pleuronectes platessa* L. *Oecologia*, 96(3):391–401, 1993.

- [84] R.A Rountree, J.P Gröger, and D Martins. Extraction of daily activity pattern and vertical migration behavior from the benthic fish, *Lophius americanus*, based on depth analysis from data storage tags. In *ICES Journal of Marine Science Symposia*, page 24, 2006.
- [85] Tristan Rouyer, Geir Ottersen, Joël M. Durant, Manuel Hidalgo, Dag Ø. Hjermann, Jonas Persson, Leif Chr. Stige, and Nils Chr. Stenseth. Shifting dynamic forces in fish stock fluctuations triggered by age truncation?: dynamic forces in fish stock fluctuations. *Global Change Biology*, 17(10):3046–3057, 2011.
- [86] J. A Sameoto and A Glass. An Overview of Discards from the Canadian Inshore Scallop Fishery in SFA 28 and SFA 29 West for 2002 to 2009. Technical report 2979, Bedford Institute of Oceanography, 2012.
- [87] B Scott, G Marteinsdottir, and P Wright. Potential effects of maternal factors on spawning stock–recruitment relationships under varying fishing pressure. *Canadian Journal of Fisheries and Aquatic Sciences*, 56:1882–1890, 1999.
- [88] W.B Scott and M.G Scott. Atlantic fishes of Canada. Technical Report 219, 1988.
- [89] Andrew Olaf Shelton, Jeffrey A. Hutchings, Robin S. Waples, David M. Keith, H. Resit Akçakaya, and Nicholas K. Dulvy. Maternal age effects on Atlantic cod recruitment and implications for future population trajectories. *ICES Journal of Marine Science*, 72(6):1769–1778, 2015.
- [90] Liese A. Siemann, Carl J. Huntsberger, Jasper S. Leavitt, and Ronald J. Smolowitz. Summering on the bank: Seasonal distribution and abundance of monkfish on Georges Bank. *PloS one*, 13(11):e0206829, 2018.
- [91] Melissa D. Smith, Jonathan H. Grabowski, and Philip O. Yund. The role of closed areas in rebuilding monkfish populations in the Gulf of Maine. *ICES Journal of Marine Science*, 65(7):1326–1333, 2008.
- [92] J Solmundsson, E Jonsson, and H Bjornsson. Recent changes in the distribution and abundance of monkfish (*Lophius piscatorius*) in Icelandic waters. In *ICES Journal of Marine Science Symposia*, page 16, 2007.
- [93] Frank W Steimle, Wallace W Morse, and Donna L Johnson. Goosefish, *lophius americanus*, life history and habitat characteristics. NOAA Technical Memorandum NMFS-NE-127, 1999.
- [94] John Stewart. Evidence of age-class truncation in some exploited marine fish populations in New South Wales, Australia. *Fisheries Research*, 108(1):209–213, 2011.
- [95] K Stokes and R Law. Fishing as an evolutionary force. *Marine Ecology-Progress Series*, 208:307–309, 2000.

- [96] Henrik Svedäng and Sara Hornborg. Selective fishing induces density-dependent growth. *Nature Communications*, 5(1):4152, 2014.
- [97] Rob Van Gemert, Ken H Andersen, and Handling editor: Jan Jaap Poos. Challenges to fisheries advice and management due to stock recovery. *ICES Journal of Marine Science*, 75(6):1864–1870, 2018.
- [98] L. Van Walraven, F.M. Mollet, C.J.G. Van Damme, and A.D. Rijnsdorp. Fisheries-induced evolution in growth, maturation and reproductive investment of the sexually dimorphic North Sea plaice (*Pleuronectes platessa* L.). *Journal of Sea Research*, 64(1-2):85–93, 2010.
- [99] Peter J. Wright and Edward A. Trippel. Fishery-induced demographic changes in the timing of spawning: consequences for reproductive success. *Fish and Fisheries*, 10(3):283–304, 2009.

## Appendix SA

This is a compilation of figures including the time-series of 1) input ( $F_{MSY}$ ) 2) average age and 3) correlogram for each stock. This file contains 172 figures. To improve readability has been made publicly available online **by clicking here**.

Figure SA1: Stock-specific time series of  $F/F_{MSY}$  and age, residuals and correlogram from analysis 2.2.2.1.

Table SA1: Relative support for linear models tested in analysis 2.2.2.3. Correlation and lag (from strongest signal) in the lower left (LL) and upper right (UR) quadrants as a function of different fixed effect predictors. df represents degrees of freedom,  $\Delta$  AICc is the relative difference in Akaike Information Criterion corrected for small sample size and r2 is the adjusted coefficient of determination from a least-squares model.

<b>Model A: LL correlation</b>	<b>df</b>	<b><math>\Delta</math>AIC</b>	<b>r<sup>2</sup></b>
cor_LL~mgmt + Order + intensity + Env + lifespan	8	69.7	-0.7415
cor_LL~mgmt + Order + intensity + Env	7	34.2	-0.5534
cor_LL~mgmt + Order + intensity + Env	6	17.4	-0.4858
cor_LL~mgmt + Order	5	6.8	-0.3273
cor_LL~mgmt + Env	4	0.3	-0.2462
cor_LL~Order + Env	5	5.8	-0.2125
cor_LL~mgmt + intensity	4	0.0	-0.217
cor_LL~mgmt + lifespan	4	0.2	-0.2389
cor_LL~mgmt + lifespan	5	7.5	-0.4156
cor_LL~mgmt + fishing	5	5.7	-0.1994
<b>Model B: LL lag</b>	<b>df</b>	<b><math>\Delta</math>AIC</b>	<b>r<sup>2</sup></b>
lag_LL~mgmt + Order + intensity + Env + lifespan	8	61.0	0.8858
lag_LL~mgmt + Order + intensity + Env	7	32.7	0.8058
lag_LL~mgmt + Order + intensity + Env	6	14.4	0.8368
lag_LL~mgmt + Order	5	5.2	0.8361
lag_LL~mgmt + Env	4	0.7	0.8144
lag_LL~Order + Env	5	25.1	-0.001
lag_LL~mgmt + intensity	4	0.0	0.8255
lag_LL~mgmt + lifespan	4	1.8	0.795
lag_LL~mgmt + lifespan	5	7.8	0.7918
lag_LL~mgmt + fishing	5	7.4	0.7998
<b>Model C: UR correlation</b>	<b>df</b>	<b><math>\Delta</math>AIC</b>	<b>r<sup>2</sup></b>
cor_UR~mgmt + Order + intensity + Env + lifespan	8	19.5	0.4274
cor_UR~mgmt + Order + intensity + Env	7	15.8	0.087
cor_UR~mgmt + Order + intensity + Env	6	11.6	-0.1216
cor_UR~mgmt + Order	5	5.8	-0.0553
cor_UR~mgmt + Env	4	2.3	-0.7753
cor_UR~Order + Env	5	2.6	0.1612
cor_UR~mgmt + intensity	4	1.6	-0.0213
cor_UR~mgmt + lifespan	4	0.0	0.0881
cor_UR~mgmt + lifespan	5	4.9	0.0112
<b>Model Dn: UR lag</b>	<b>df</b>	<b><math>\Delta</math>AIC</b>	<b>r<sup>2</sup></b>
Lag_UR~mgmt + Order + intensity + Env + lifespan	8	25.5	0.1389
lag_UR~mgmt + Order + intensity + Env	7	14.9	0.1592
lag_UR~mgmt + Order + intensity + Env	6	8.1	0.1474
lag_UR~mgmt + Order	5	1.6	0.2337
lag_UR~mgmt + Env	4	3.3	-0.1288
lag_UR~Order + Env	5	2.4	0.1906
lag_UR~mgmt + intensity	4	0.0	0.1088
lag_UR~mgmt + lifespan	4	3.3	-0.13
lag_UR~mgmt + lifespan	5	8.4	-0.2415



Table SA2: Results from the prewhitened cross-correlations (analysis 2.2.2.1). The upper 90 % C.I. value, correlation (cor), lag and significance (sig) per quadrant (UR= upper right, LR= lower right, UL= upper left, LL= lower left) and ARIMA orders (p,d,q) are represented for each stock.

Unique ID	upperCI	cor_UR	lag_UR	sig_UR	cor_LR	lag_LR	sig_LR	cor_UL	lag_UL	sig_UL	cor_LL	lag_LL	sig_LL	orderP	orderD	orderQ
ICES-WGBFAS_harengus_BS 28.1	0.2668305	0.170793	7	FALSE	-0.22986	1	FALSE	0.182822	-7	FALSE	-0.28968	-3	TRUE	1	0	0
ICES-WGBFAS_harengus_BS 25-29,32	0.256883	0.17112	12	FALSE	-0.17241	7	FALSE	0.18509	-13	FALSE	-0.27188	-2	TRUE	1	0	0
NEFSC-GARMIII_cynoglossus_5Y	0.2820901	0.060697	6	FALSE	-0.13849	5	FALSE	0.152223	-7	FALSE	-0.21114	-11	FALSE	2	0	0
ICES-WGWIDE_poutassou_NEA 1-9,12,14	0.2668305	0.331951	8	TRUE	-0.1962	6	FALSE	0.263765	-5	FALSE	-0.15377	-7	FALSE	2	0	0
ICES-WGWIDE_harengus_NEA 1,2,5,4a,14a	0.2954244	0.337422	7	TRUE	-0.30901	4	TRUE	0.202341	-7	FALSE	-0.16697	-1	FALSE	4	0	0
NEFSC_americanus_SZ	0.2907718	0.293207	1	TRUE	-0.28817	8	FALSE	0.297698	-9	TRUE	-0.28001	-11	FALSE	0	1	0
ICES-WGBFAS_spratrus_BS 22-32	0.256883	0.313359	7	TRUE	-0.25292	6	FALSE	0.204417	-2	FALSE	-0.13142	-9	FALSE	0	1	0
ICES-WGNSSK_solea_NS 7d.	0.5201484	0.394963	1	FALSE	-0.13518	4	FALSE	0.126123	-5	FALSE	-0.34794	-6	FALSE	0	1	0
ICES-WGNSSK_merlangus_NS 4-7d	0.3165522	0.348895	3	TRUE	-0.27698	1	FALSE	0.218309	-3	FALSE	-0.20662	-6	FALSE	0	1	0
ICES-HAWG_harengus_NS-IV 3a,7d	0.1965976	0.33679	15	TRUE	-0.36552	14	TRUE	0.116372	-5	FALSE	-0.16298	-6	FALSE	0	1	0
NEFSC-TRAC-CERT_morhua_GB	0.2668305	0.255311	8	FALSE	-0.25395	7	FALSE	0.215326	-10	FALSE	-0.25685	-3	FALSE	0	1	0
ICES-WGBFAS_solea_NS IIIa 22-24	0.2954244	0.323118	11	TRUE	-0.3581	6	TRUE	0.257548	-8	FALSE	-0.17344	-3	FALSE	0	1	0
NEFSC_macrocephalus_BSAI	0.256883	0.181007	9	FALSE	-0.19122	1	FALSE	0.214853	-5	FALSE	-0.2464	-2	FALSE	0	1	0
NEFSC_scombrus_NWA	0.2349791	0.269579	11	TRUE	-0.2084	9	FALSE	0.14857	-4	FALSE	-0.19972	-2	FALSE	0	1	0
NEFSC-SAW_morhua_GOM	0.3003078	0.311323	2	TRUE	-0.20388	5	FALSE	0.191721	-11	FALSE	-0.28852	-1	FALSE	0	1	0
ICES-WGSCSE_solea_CS7f,7g	0.2425204	0.334905	1	TRUE	-0.27044	4	TRUE	0.292051	-8	TRUE	-0.23828	-1	FALSE	0	1	0
NEFSC_platessoides_5YZ	0.2633874	0.294257	3	TRUE	-0.28633	7	TRUE	0.207817	-7	FALSE	-0.27488	-10	TRUE	0	1	0
NEFSC-GARMIII_aeglefinus_5Y	0.2704123	0.137506	5	FALSE	-0.06822	11	FALSE	0.159128	-5	FALSE	-0.31612	-9	TRUE	0	1	0
NEFSC-GARMIII_dentatus_MA	0.2954244	0.404032	7	TRUE	-0.25919	6	FALSE	0.104676	-4	FALSE	-0.31636	-6	TRUE	0	1	0
NEFSC-GARMIII_tenuis_GOM_GB	0.2349791	0.308872	9	TRUE	-0.23718	3	TRUE	0.292089	-8	TRUE	-0.28373	-6	TRUE	0	1	0
ICES-WGSCSE_platessa_I527-7a	0.2741423	0.168073	7	FALSE	-0.07997	10	FALSE	0.253605	-11	FALSE	-0.30652	-4	TRUE	0	1	0
NEFSC-SAW_chrysops_USATL	0.2954244	0.216375	2	FALSE	-0.12954	6	FALSE	0.298698	-9	TRUE	-0.45154	-3	TRUE	0	1	0
ICES-HAWG_harengus_WBS 22-24	0.3289707	0.173854	4	FALSE	-0.2274	10	FALSE	0.147146	-8	FALSE	-0.47733	-2	TRUE	0	1	0
ICES-WGSCSE_solea_I57e	0.2374142	0.228061	3	FALSE	-0.20879	5	FALSE	0.165257	-4	FALSE	-0.3407	-2	TRUE	0	1	0
ICES-WGNSSK_aeglefinus_NS 4-6a-20	0.247971	0.199435	2	FALSE	-0.22282	4	FALSE	0.267607	-5	TRUE	-0.34571	-3	TRUE	2	1	0
ICES-NWWG_virens_FA5b	0.2198028	0.243553	12	TRUE	-0.07722	5	FALSE	0.383215	-6	TRUE	-0.345	-1	TRUE	2	1	0
ICES-AFWG_morhua_NEA 1,2	0.1952082	0.247608	7	TRUE	-0.19643	2	TRUE	0.139266	-8	FALSE	-0.26838	-4	TRUE	3	1	0
ICES-WGNSSK_platessa_NS 7d	0.2704123	0.303849	1	TRUE	-0.28573	5	TRUE	0.146467	-2	FALSE	-0.31003	-3	TRUE	3	1	0
ICES-WGNSSK_platessa_NS 4,20	0.2123497	0.262207	1	TRUE	-0.2065	2	FALSE	0.287895	-4	TRUE	-0.31535	-5	TRUE	2	2	0
ICES-HAWG_harengus_CS 6a,7b,7c	0.2141417	0.368317	7	TRUE	-0.2354	6	TRUE	0.115976	-6	FALSE	-0.17744	-12	FALSE	0	1	1
ICES-WGSCSE_morhua_I57a	0.2349791	0.252837	1	TRUE	-0.2149	3	FALSE	0.215059	-8	FALSE	-0.20943	-3	FALSE	0	1	1
NEFSC-GARMIII_morhua_GB	0.2820901	0.377008	1	TRUE	-0.45552	7	TRUE	0.239013	-10	FALSE	-0.33645	-7	TRUE	0	1	1
AFSC_aspera_EEBSAI	0.2508378	0.160037	6	FALSE	-0.24919	4	FALSE	0.251211	-5	TRUE	-0.36701	-4	TRUE	0	1	1
ICES-WGNSSK_virens_NS 4,6,3a	0.2326174	0.222112	3	FALSE	-0.14895	7	FALSE	0.382732	-3	TRUE	-0.35937	-2	TRUE	0	1	1
CERT-TRAC_aeglefinus_GB	0.2374142	0.196101	1	FALSE	-0.17056	12	FALSE	0.20233	-9	FALSE	-0.29445	-8	TRUE	3	1	1
NEFSC_virens_5YZ	0.247971	0.247061	2	FALSE	-0.17229	1	FALSE	0.135684	-4	FALSE	-0.15493	-12	FALSE	0	1	2
ICES-WGSCSE_aeglefinus_ROCK6b	0.3225823	0.287482	4	FALSE	-0.44077	1	TRUE	0.416831	-11	TRUE	-0.15124	-6	FALSE	0	1	2
ICES-WGSCSE_morhua_CS7e-k	0.2425204	0.347711	1	TRUE	-0.24038	4	FALSE	0.164382	-7	FALSE	-0.1784	-4	FALSE	0	1	2
NEFSC-GARMIII_ferruginea_SNE, MA	0.2633874	0.179402	10	FALSE	-0.19894	1	FALSE	0.248526	-7	FALSE	-0.32049	-8	TRUE	0	1	2
ICES-NWWG_morhua_FAPLSb1	0.2178662	0.312785	1	TRUE	-0.27813	14	TRUE	0.196725	-9	FALSE	-0.30637	-5	TRUE	3	1	2
ICES-WGSCSE_merlangus_CS7a	0.2704123	0.208128	12	FALSE	-0.28838	9	TRUE	0.164984	-8	FALSE	-0.12588	-7	FALSE	0	1	3
ICES-AFWG_aeglefinus_NEA 1,2	0.1994678	0.208792	3	TRUE	-0.15826	2	FALSE	0.148026	-7	FALSE	-0.12336	-6	FALSE	0	1	3
AFSC_polyxystra_EEBSAI-Females	0.2704123	0.093363	11	FALSE	-0.23904	3	FALSE	0.27845	-5	TRUE	-0.16295	-10	FALSE	0	1	4

Table SA3: Details for prewhitened cross-correlation analysis 2.2.2.1.

Step	Notes
Examine input and output time series	<code>plot.ts()</code> function from TSA package
Define ARIMA orders (p,d,q), fit the model and inspect performance	<code>auto.arima()</code> function from Forecast package
Apply fitted model to input and output	<pre>prewhite_input&lt;-input - fitted(Arima(input, model = arima_model)) prewhite_output&lt;-output - fitted(Arima(output, model = arima_model))</pre> <p>*arima_model defined in step B</p>
Cross-correlation between the treated series	<code>ccf&lt;-ccf(prewhite_input, prewhite_output)</code>
Extract strongest signal (max absolute correlation) from each quadrant and determine significance level	<pre>cor&lt;-ccf\$acf lag&lt;-ccf\$lag</pre>

## Appendix SB

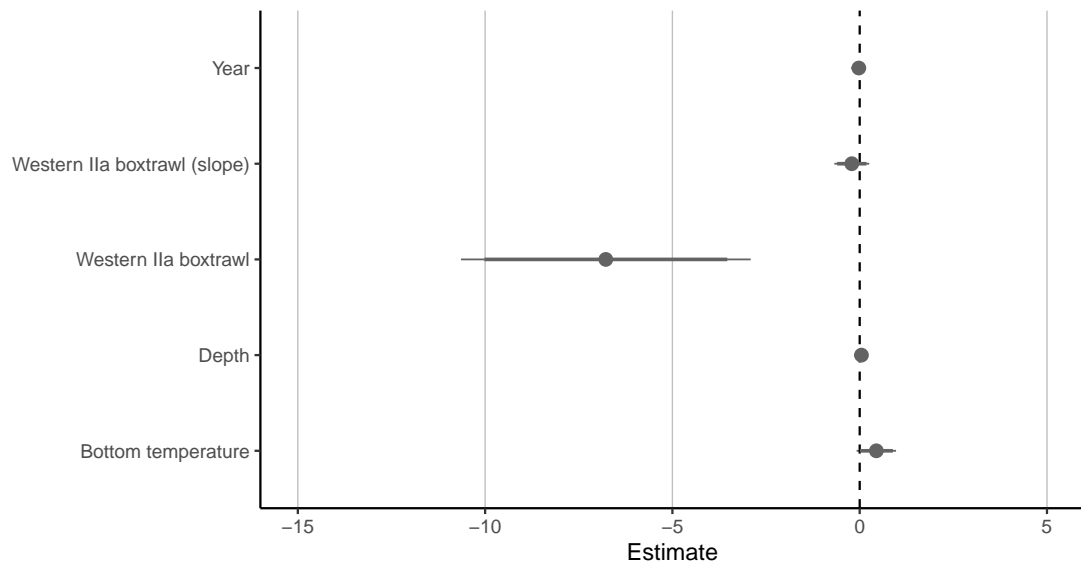


Figure SB1: Effect size plot from a linear model analysis of monkfish length frequencies  $n=678$  for the US-Canada bottom trawl survey comparison (equation2) (US: Yankee trawl, Canada: Western IIA trawl). Circles represent the estimates, thick and thin bars represent 90 % and 95 % uncertainty intervals, respectively. Positive values correspond to increased length relative to the baseline gear type (i.e. Yankee trawl). Year centered at 2007

Table SB1: Estimated regression parameters, standard errors and t-values for the mixed effects model presented in equation 1. Baselines for gear type = Yankee trawl and for season = summer. The estimated value for  $\sigma_{Year}=0.06128$  and  $\sigma_{Area}=49.44346$ .

	<b>Estimate</b>	<b>Std. Error</b>	<b>t-value</b>
<b>(Intercept)</b>	59.933286	2.294786	26.177
<b>Year</b>	-0.614710	0.079479	-7.734
<b>Scallop dredge</b>	-14.312713	1.233963	-11.599
<b>Western IIA trawl</b>	-5.024570	2.514309	-1.988
<b>Modified Yankee trawl</b>	0.27051	1.298082	0.208
<b>Fall</b>	-5.181575	0.543795	-9.529
<b>Spring</b>	-2.869576	0.542629	-5.288
<b>Bottom temperature</b>	0.800649	0.075693	10.578
<b>Depth</b>	0.018071	0.003392	5.327
<b>Scallop dredge slope</b>	0.204783	0.053476	3.829
<b>Western IIA trawl slope</b>	-0.058070	0.091648	-0.634
<b>Yankee trawl slope</b>	0.233105	0.256378	0.909

Table SB2: Estimated regression parameters, standard errors, t-values and p-values for the linear model presented in equation 2. Baseline gear type = Yankee trawl.

	<b>Estimate</b>	<b>Std. Error</b>	<b>t-value</b>	<b>Pr(&gt; t )</b>
<b>(Intercept)</b>	45.6959	0.67757	67.441	< 2.00e-16***
<b>Year</b>	-0.04731	0.07738	-0.611	0.54112
<b>Western IIA trawl</b>	-6.24264	1.87478	-3.33	0.000917***
<b>Depth</b>	0.04753	0.01014	4.687	3.36E-06***
<b>Bottom temperature</b>	0.41931	0.26672	1.572	0.116401

Table SB3: Relative support for linear models tested for the US-Canada bottom trawl survey comparison (equation 2). Monkfish length (cm) as a function of different fixed effect predictors, where df represents degrees of freedom, LogLik is the log likelihood,  $\Delta$  AIC is the relative difference in Akaike Information Criterion,  $w_i$  are the Akaike weights and  $r^2$  is the coefficient of determination from a least-squares model.

<b>Model</b>	<b>df</b>	<b>LogLik</b>	<b><math>\Delta</math>AIC</b>	<b><math>w_i</math></b>	<b><math>r^2</math></b>
length~year + surveygear + depth + bottomtemp	6		0	6.44e-01	0.1015
length~year + year*surveygear + depth + bottomtemp	7		1.44	3.14e-01	0.1023
length~year + surveygear + depth	5		5.50	4.13e-02	0.09156
length~year + surveygear + bottomtemp	5		17.73	9.12e-05	0.07502